

**Azacalix[2]arene[2]triazine-based receptors bearing carboxymethyl
pendant arms on nitrogen bridges: synthesis and evaluation of their
coordination ability towards copper(II)**

**João M. Caio,^{a,b} Teresa Esteves,^b Silvia Carvalho,^a Cristina Moiteiro^{*b} and Vítor
Félix^{*a}**

Contents

¹ H and ¹³ C NMR Spectra.....	2
Infrared spectra	11
Mass Spectra.....	14
UV-vis Titration	25
Crystallographic data.....	28

^1H and ^{13}C NMR Spectra

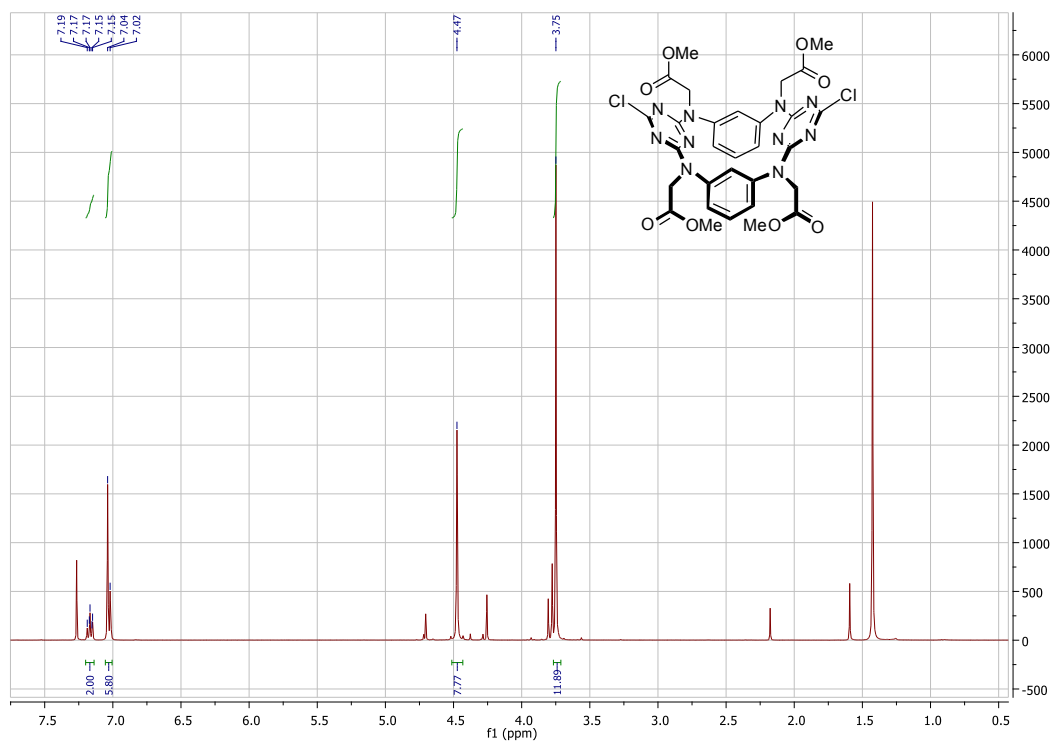


Figure S1. ^1H NMR spectrum of **1** (CDCl_3 , 400 MHz).

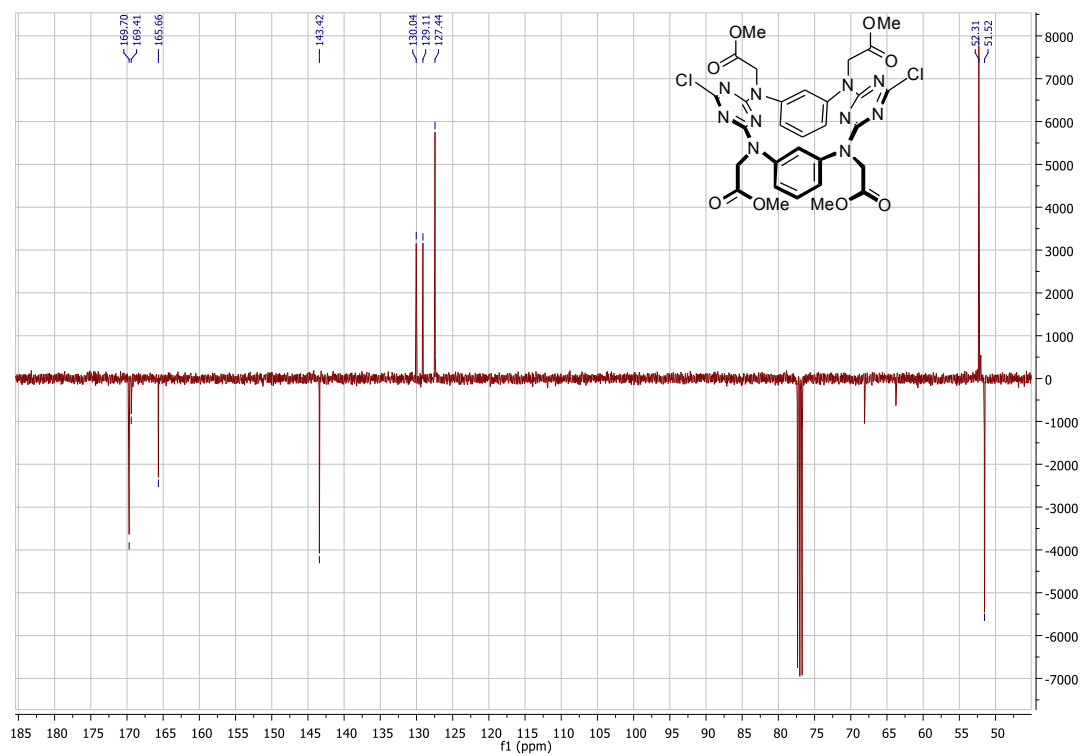


Figure S2. ^{13}C NMR spectrum of **1** (CDCl_3 , 101 MHz).

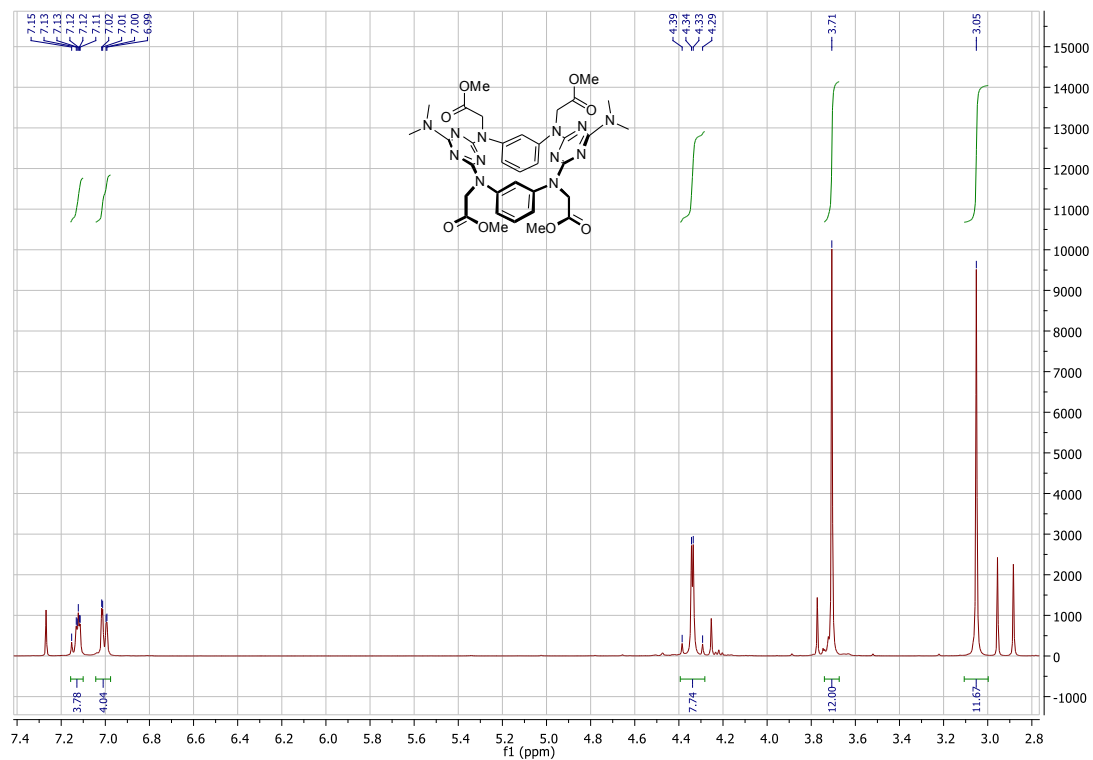


Figure S3. ^1H NMR spectrum of **2** (CDCl_3 , 400 MHz).

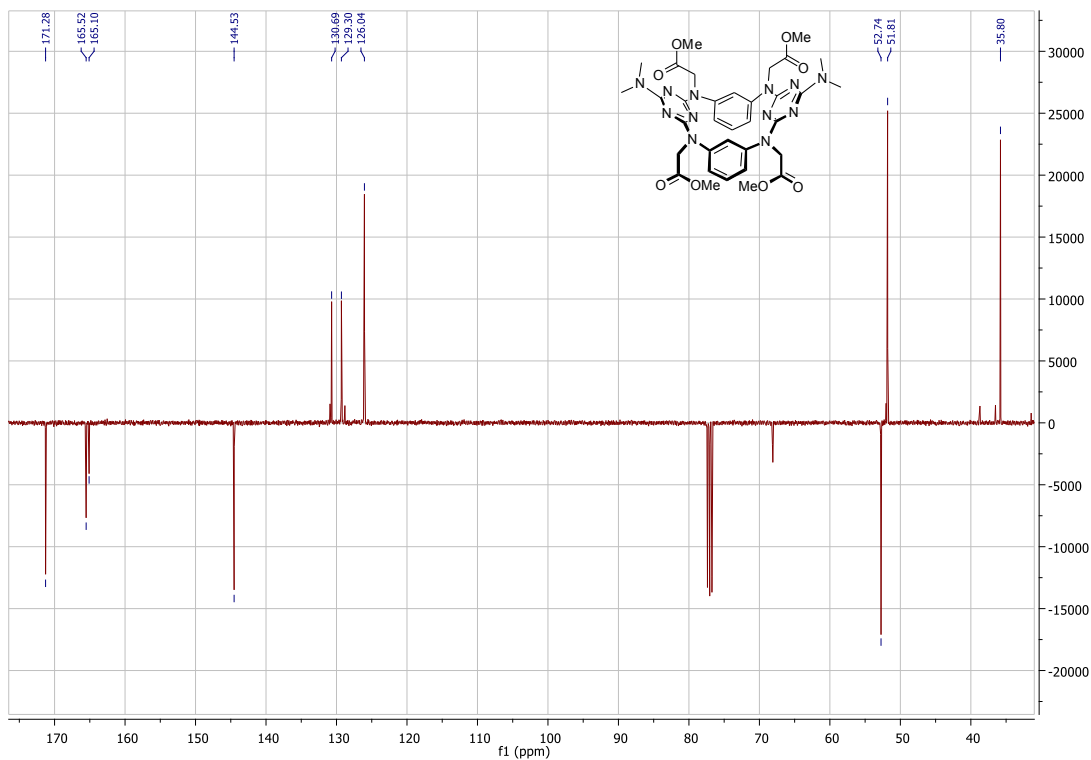


Figure S4. ^{13}C NMR spectrum of **2** (CDCl_3 , 101 MHz).

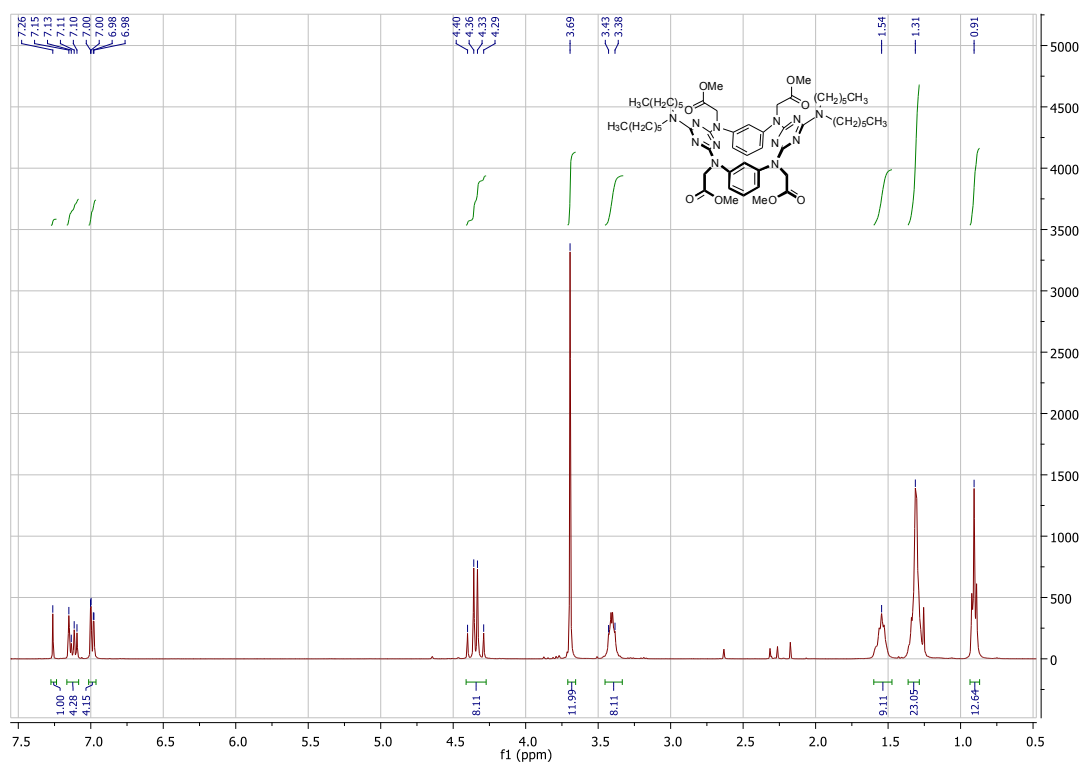


Figure S5. ^1H NMR spectrum of **3** (CDCl_3 , 400 MHz).

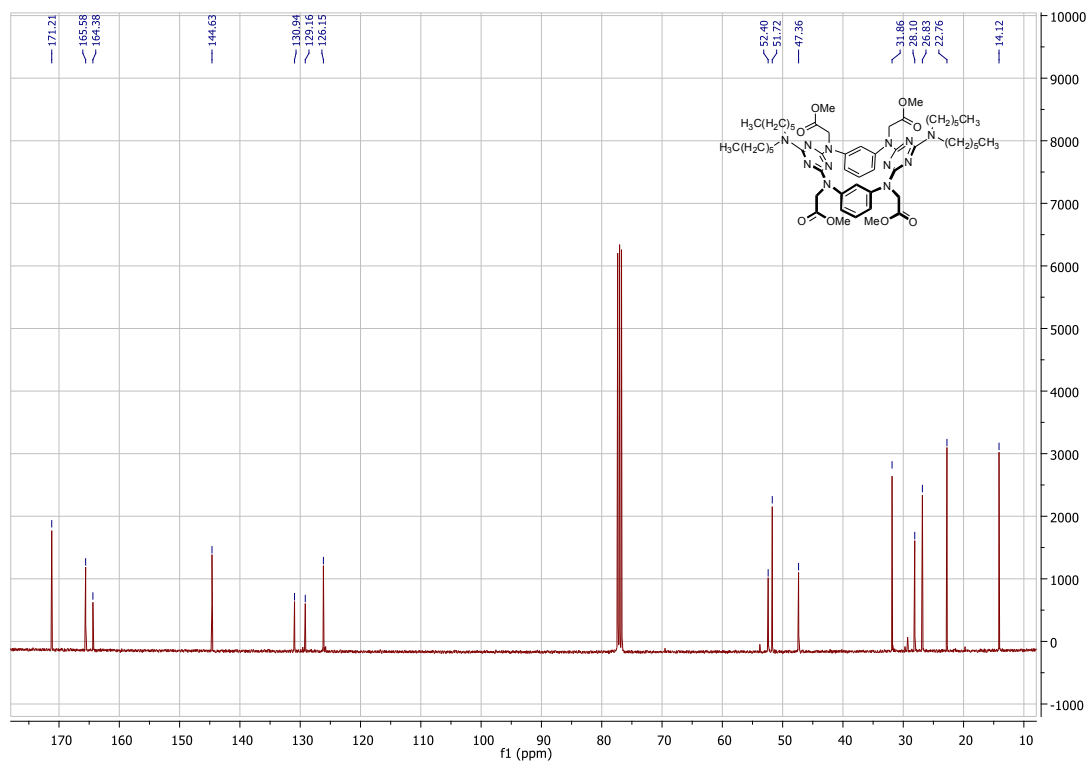


Figure S6. ^{13}C NMR spectrum of **3** (CDCl_3 , 101 MHz).

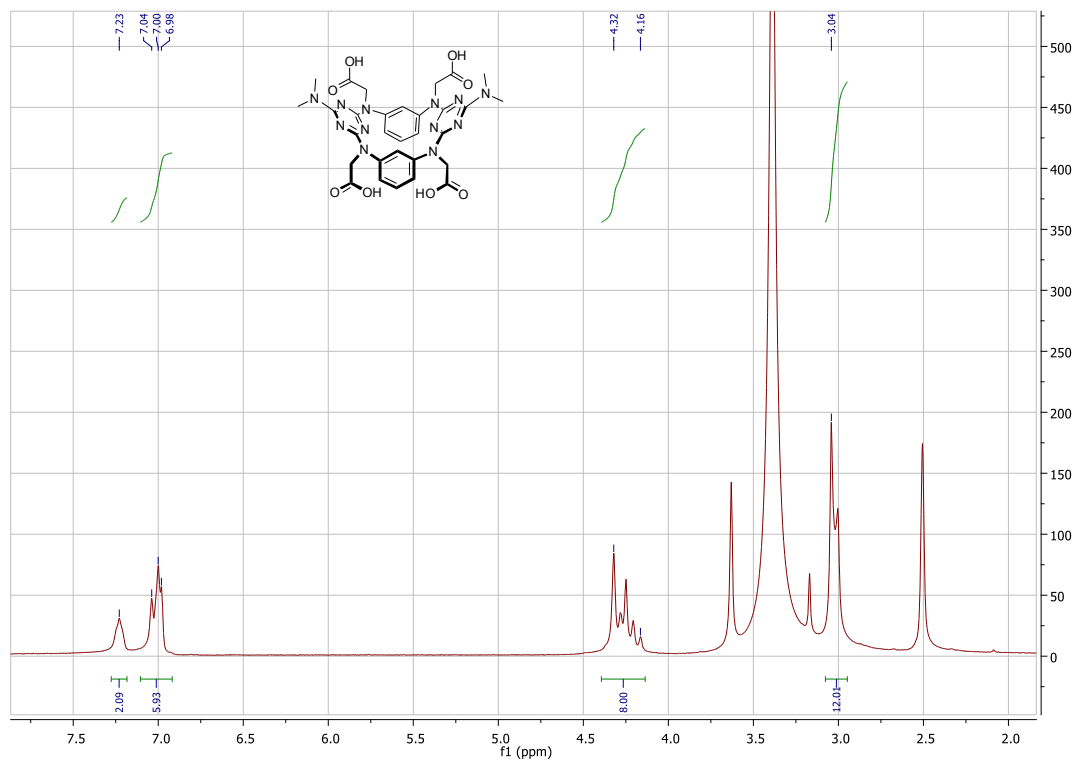


Figure S7. ^1H NMR spectrum of 4 (DMSO, 400 MHz).

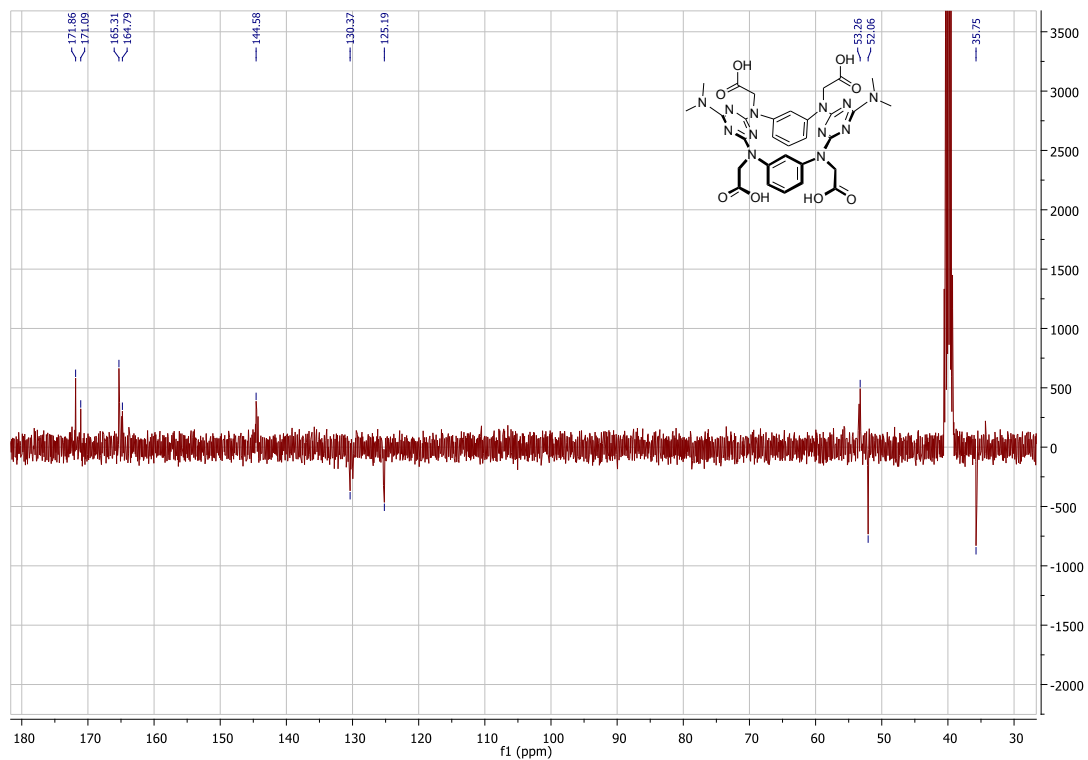


Figure S8. ^{13}C NMR spectrum of 4 (DMSO, 101 MHz).

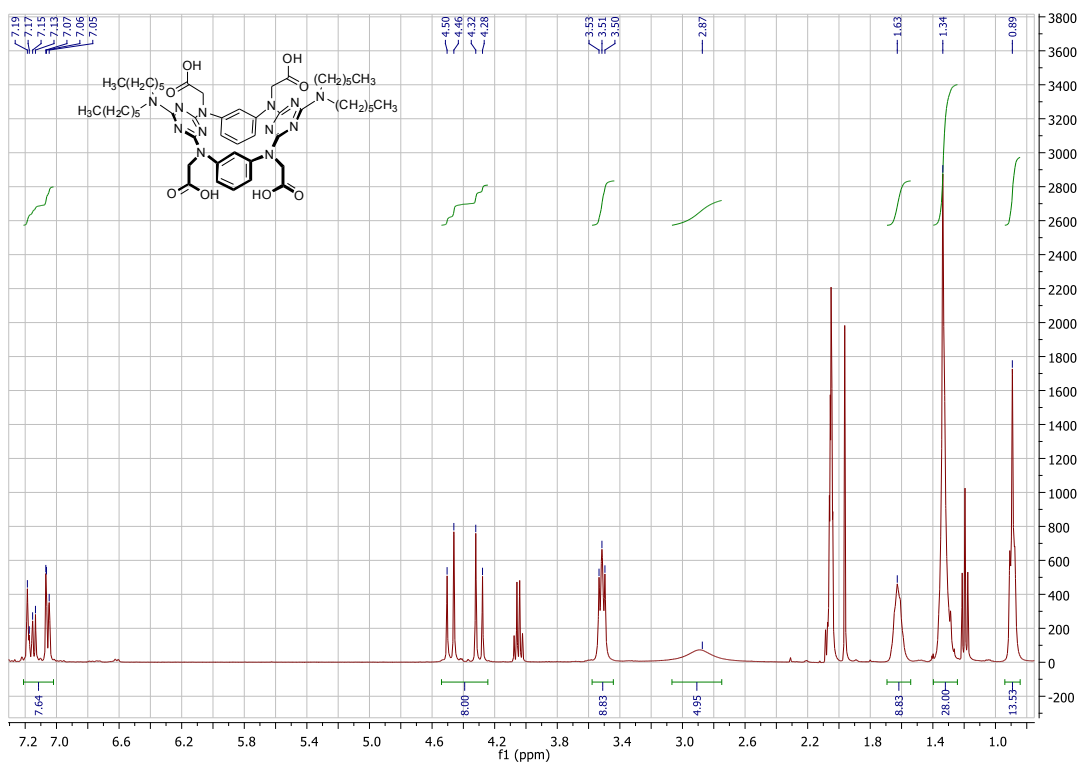


Figure S9. ^1H NMR spectrum of **5** (acetone, 400 MHz).

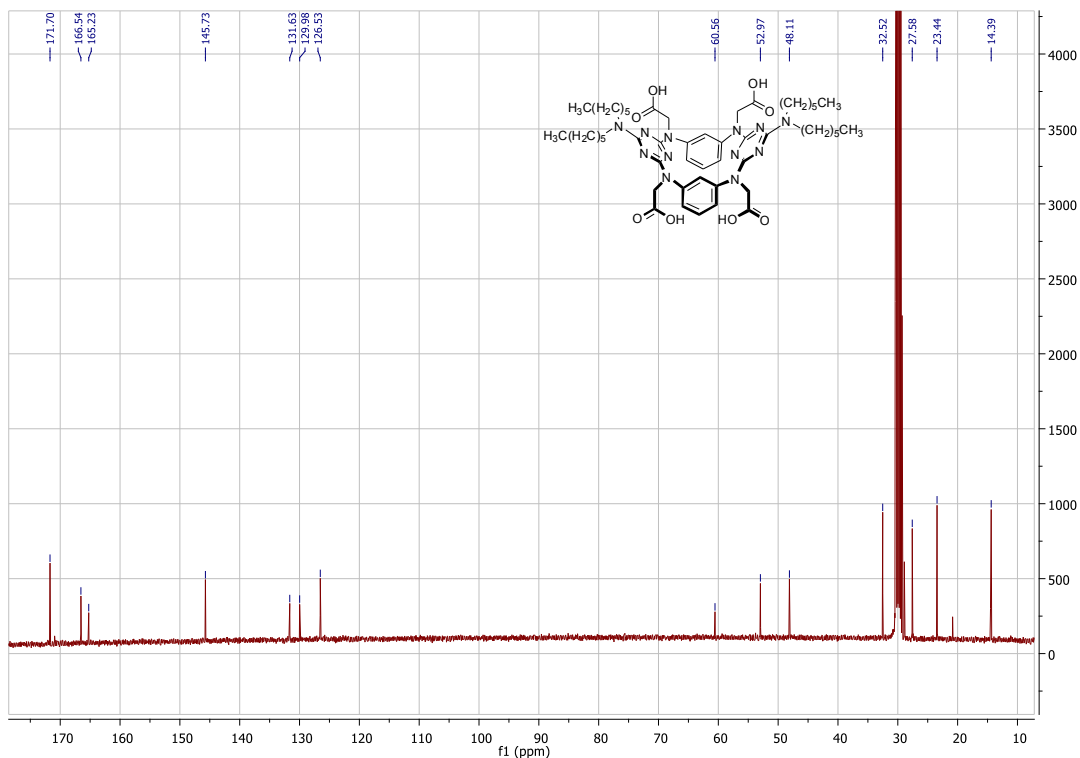


Figure S10. ^{13}C NMR spectrum of **5** (acetone, 101 MHz).

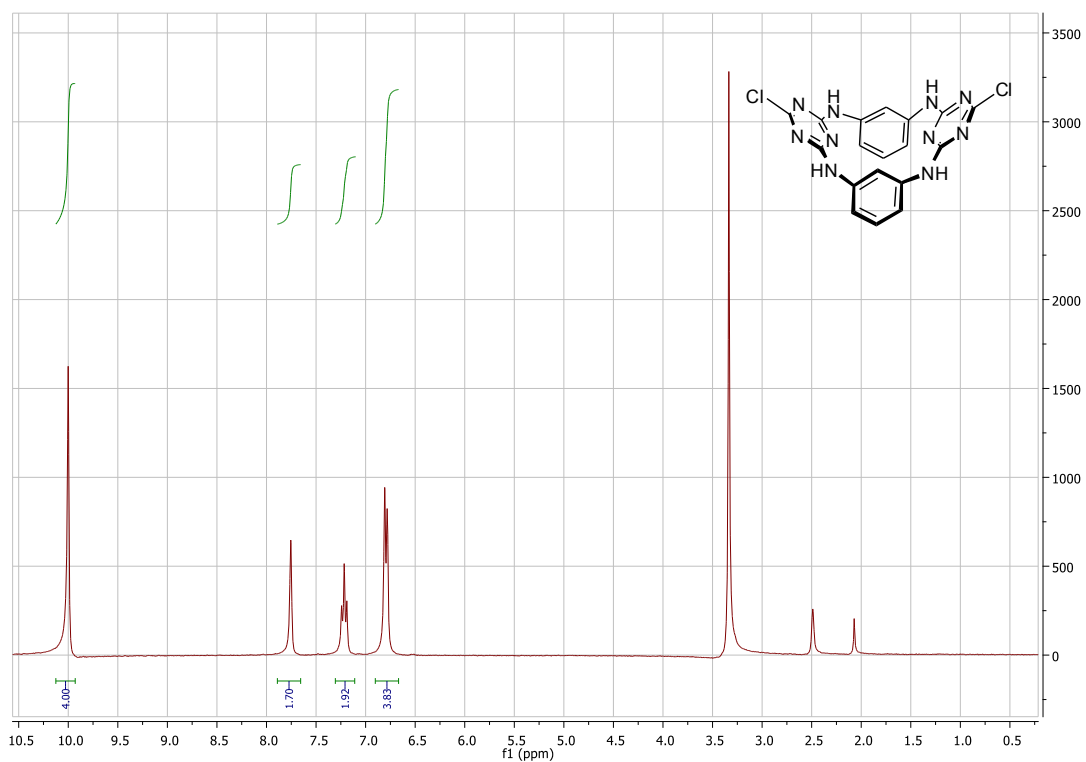


Figure S11. ^1H NMR spectrum of **10** (DMSO, 400 MHz).

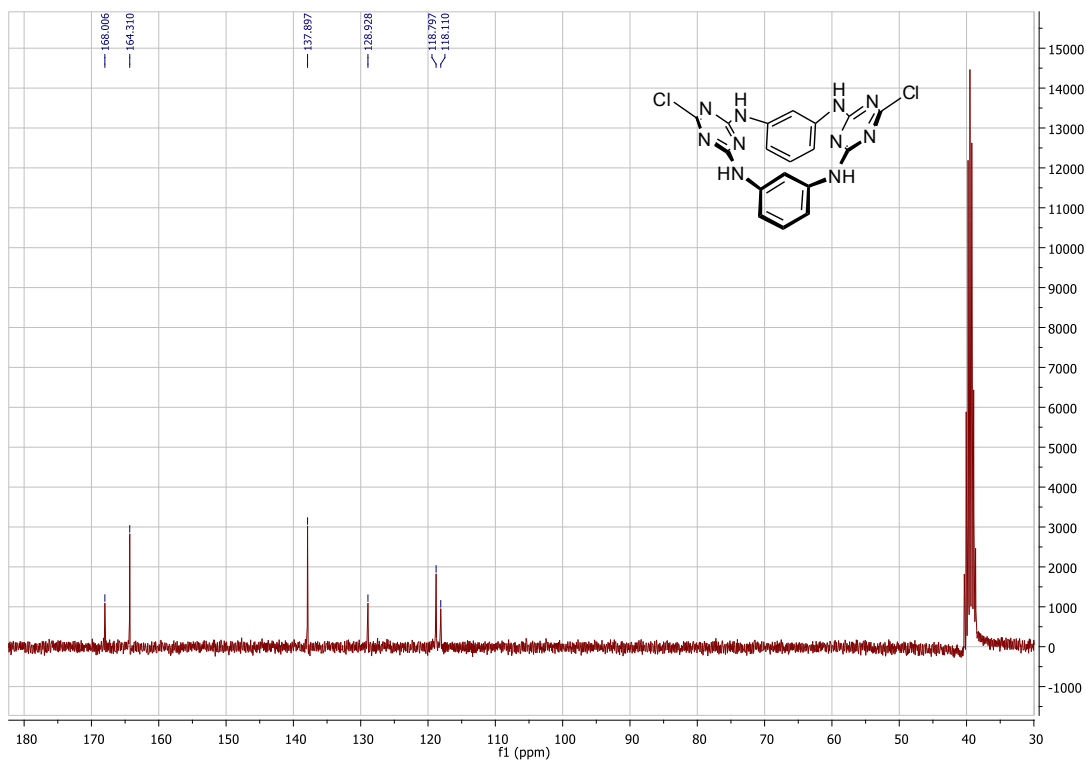


Figure S12. ^{13}C NMR spectrum of **10** (DMSO, 101 MHz).

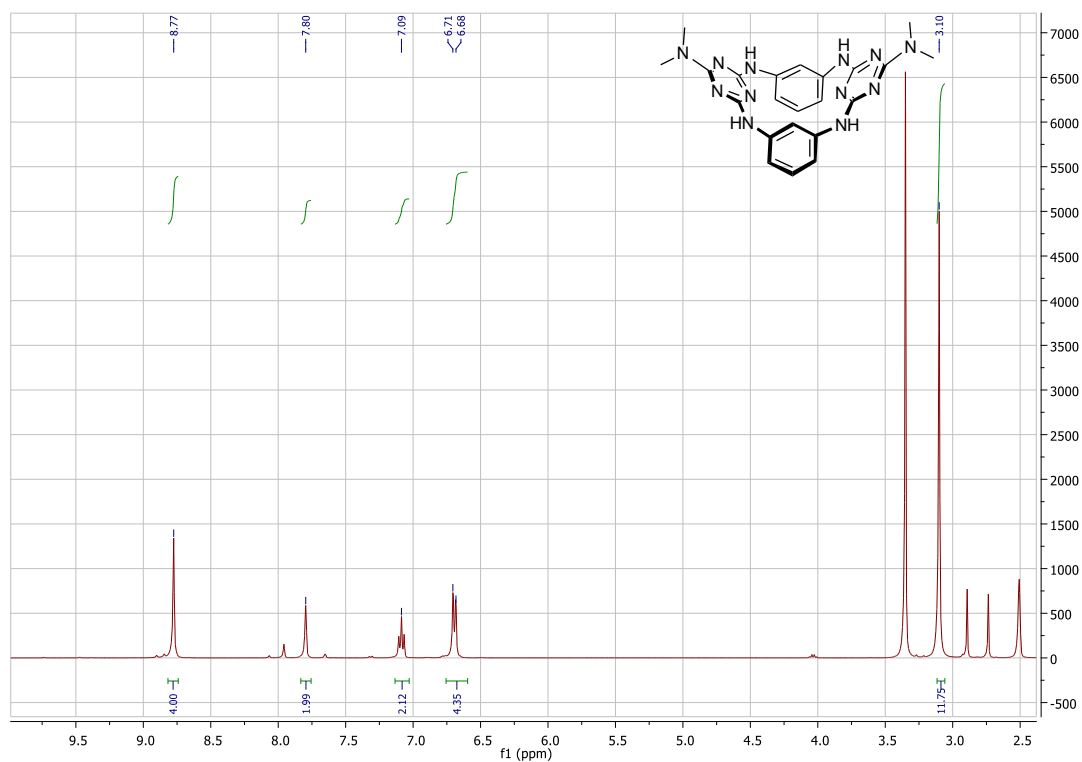


Figure S13. ^1H NMR spectrum of **11** (DMSO, 400 MHz).

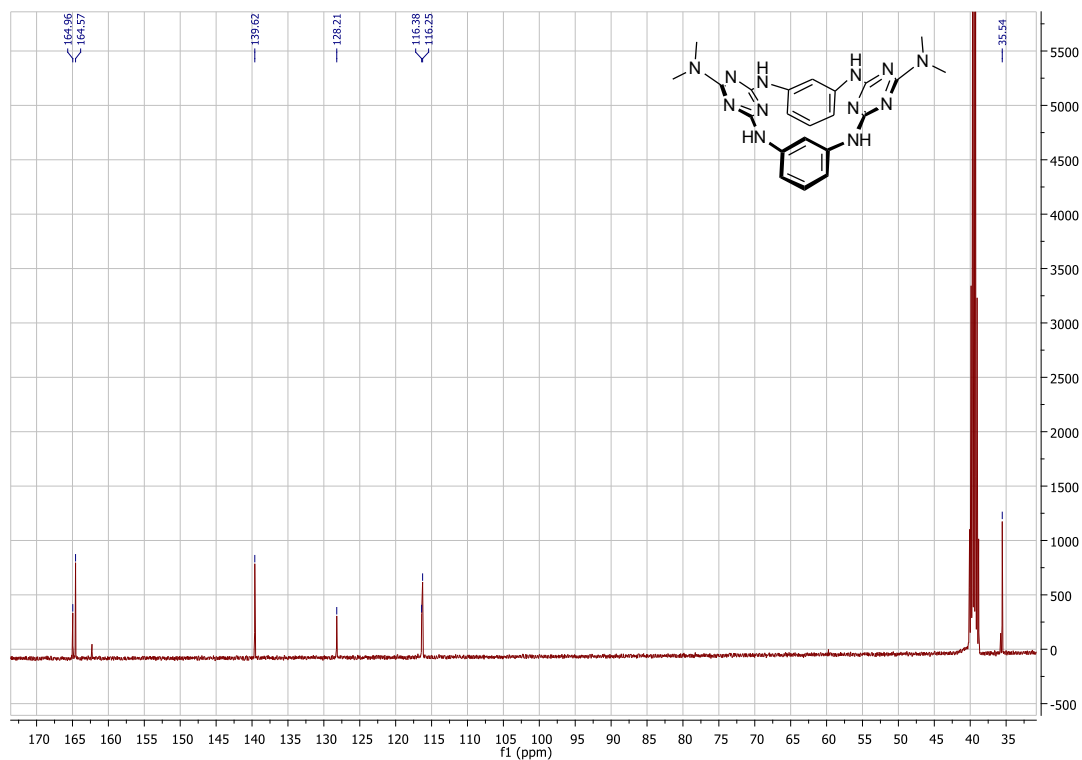


Figure S14. ^{13}C NMR spectrum of **11** (DMSO, 101 MHz).

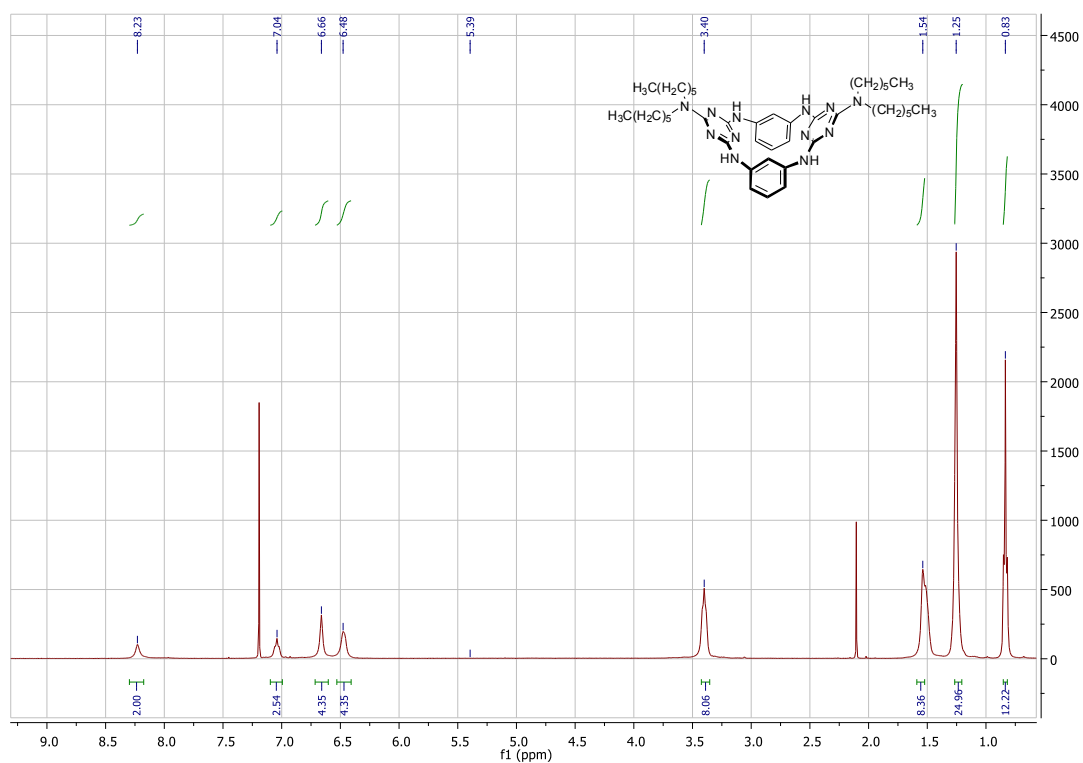


Figure S15. ^1H NMR spectrum of **12** (CDCl_3 , 400 MHz).

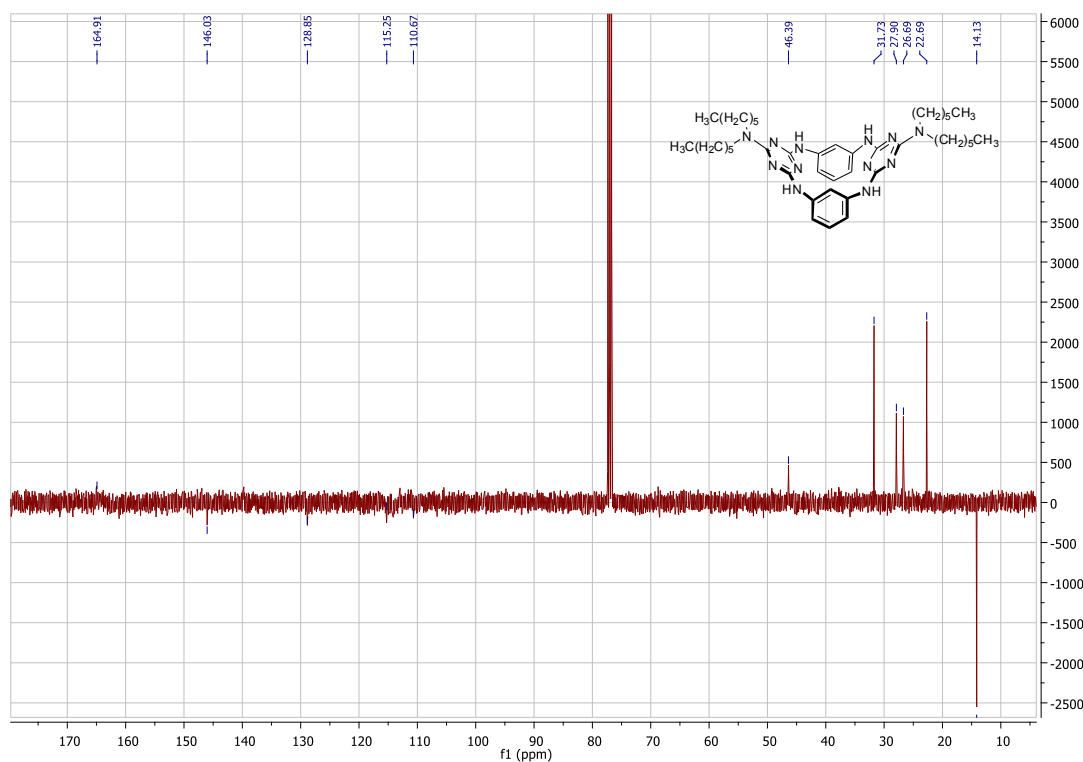


Figure S16. ^{13}C NMR spectrum of **12** (CDCl_3 , 101 MHz).

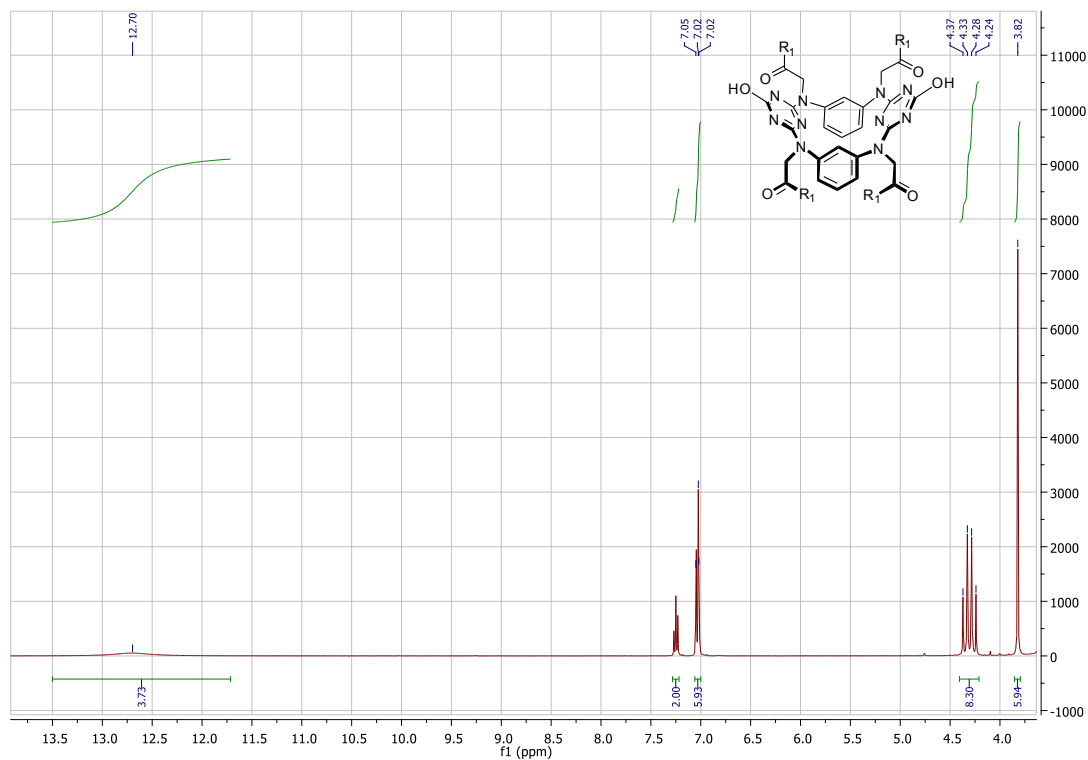


Figure S17. ^1H NMR spectrum of **13** (DMSO, 400 MHz).

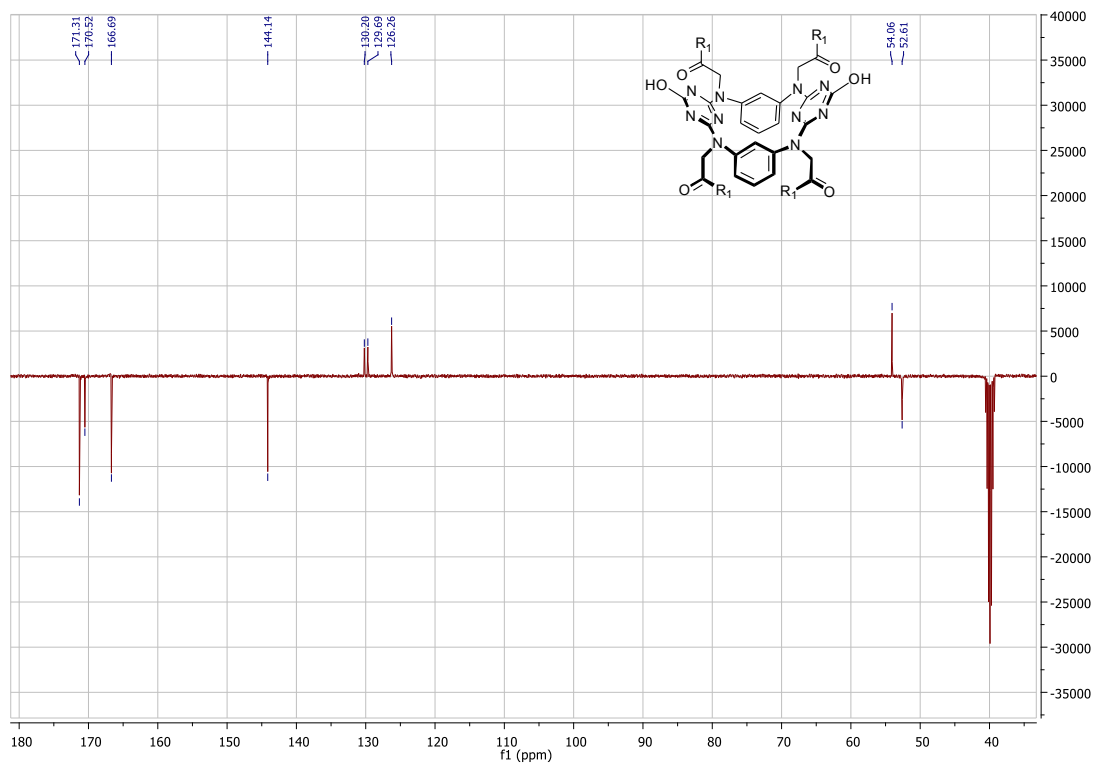


Figure S18. ^{13}C NMR spectrum of **13** (DMSO, 101 MHz).

Infrared spectra

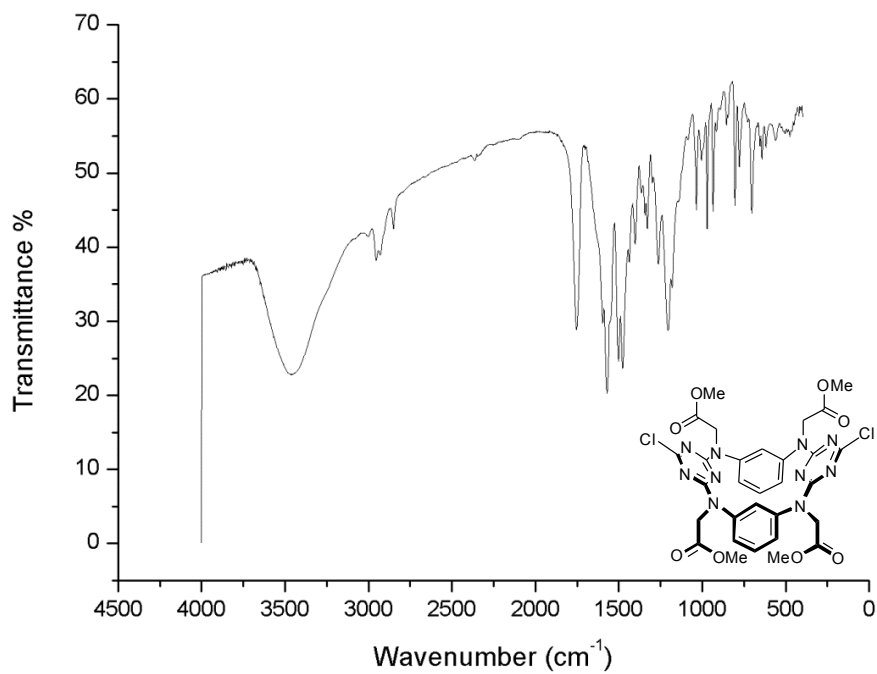


Figure S19. Infrared spectrum of 1.

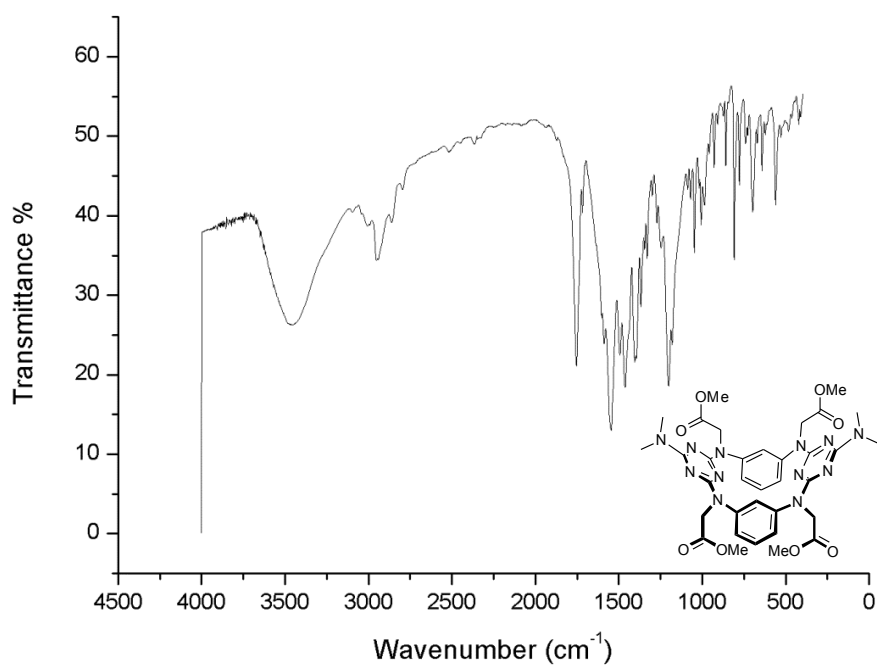


Figure S20. Infrared spectrum of 2.

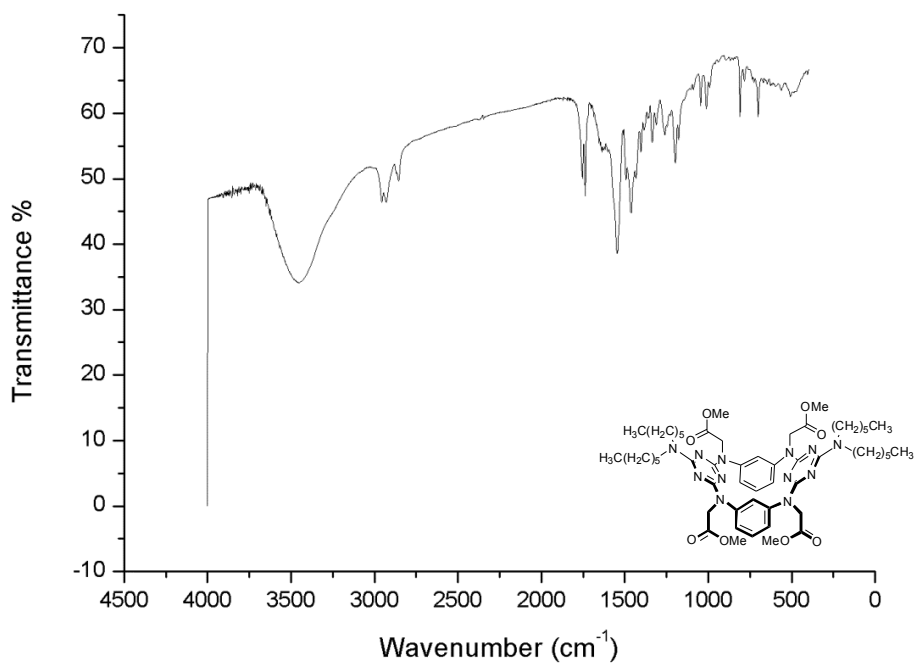


Figure S21. Infrared spectrum of 3.

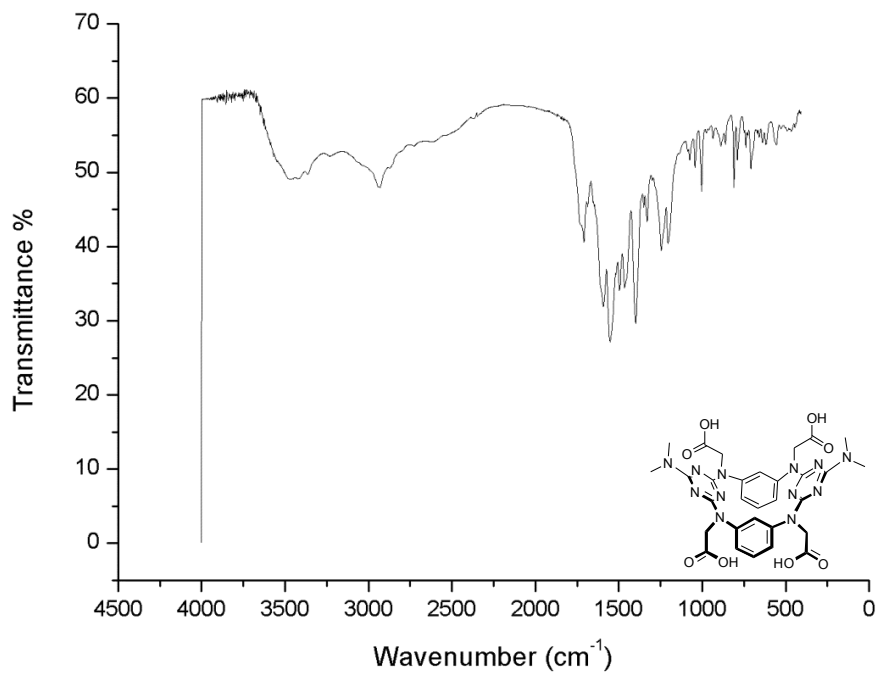


Figure S22. Infrared spectrum of 4.

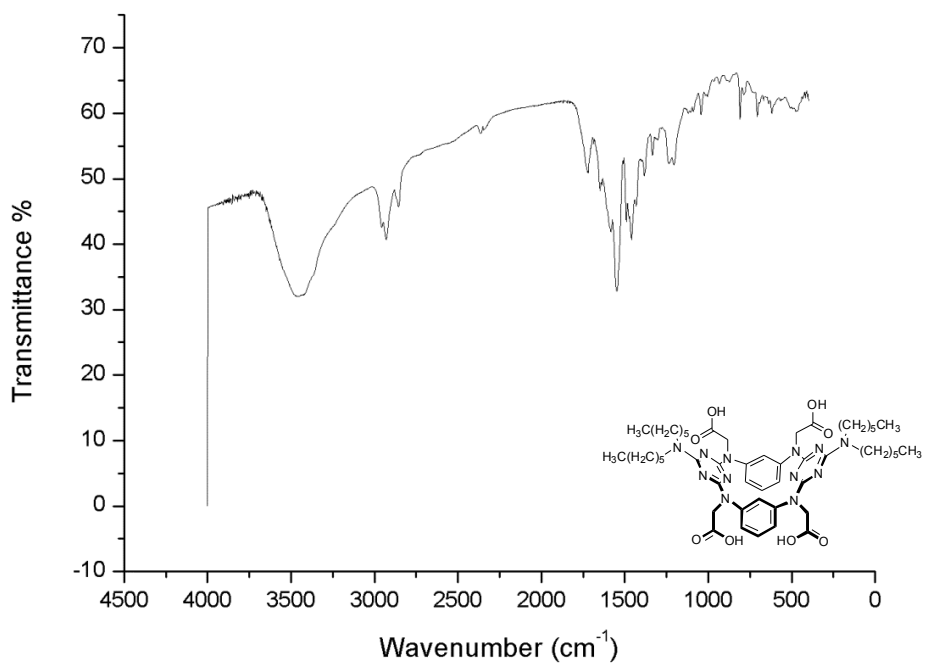


Figure S23. Infrared spectrum of **5**.

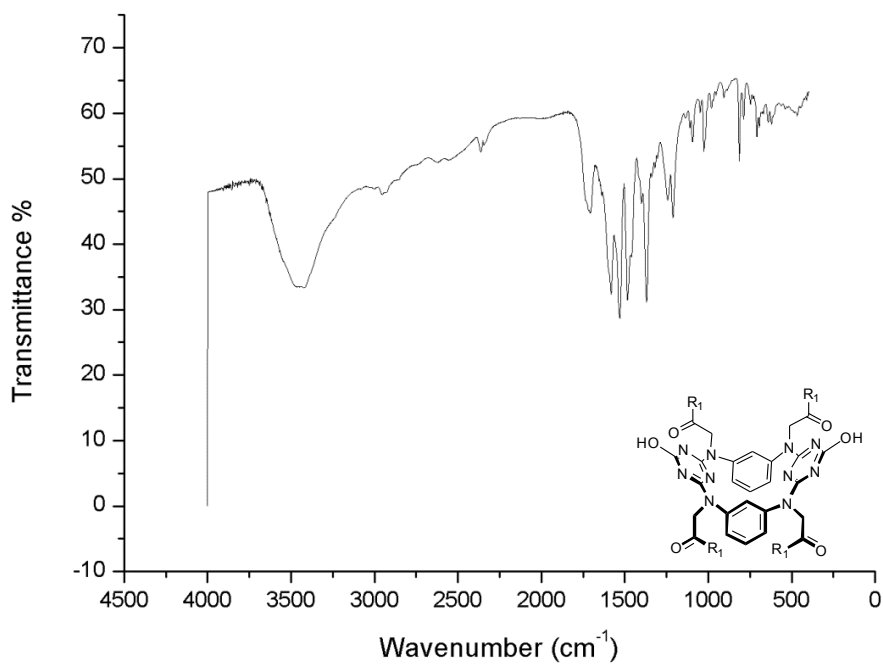


Figure S24. Infrared spectrum of **13**.

Mass Spectra

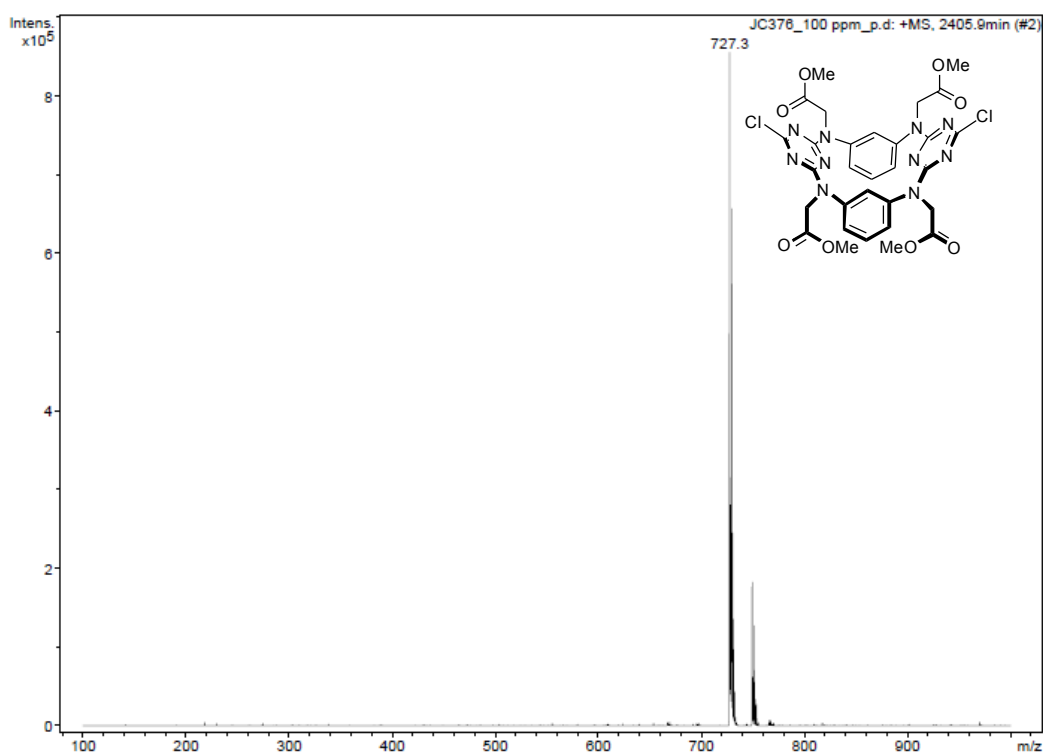


Figure S25. MS (ESI) spectrum of 1.

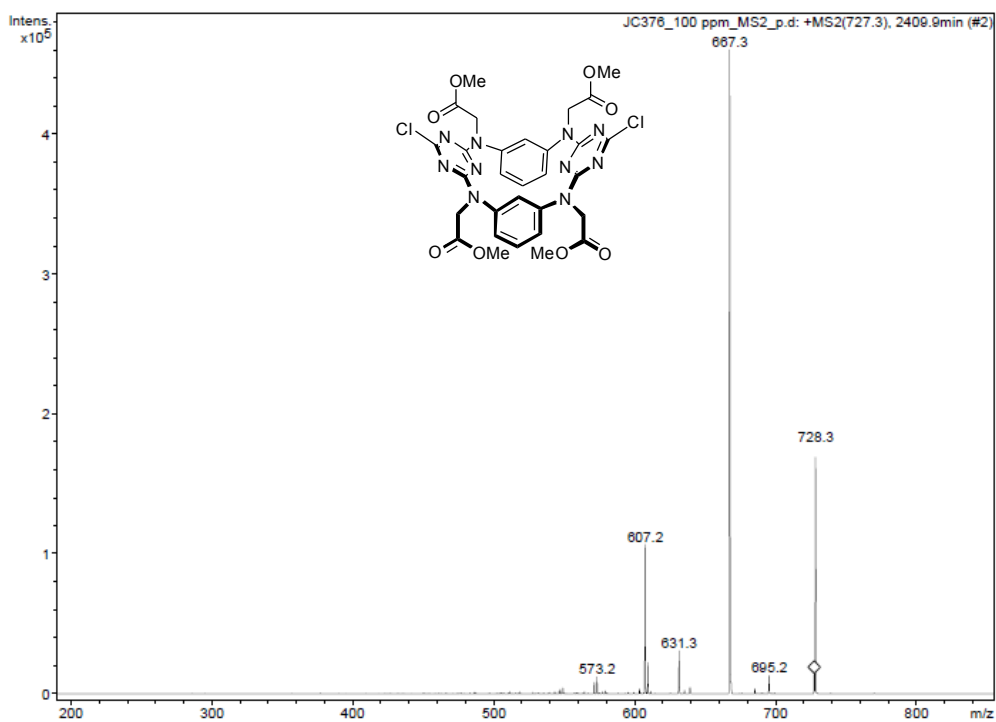


Figure S26. MS² spectrum of the [M+H]⁺ of 1.

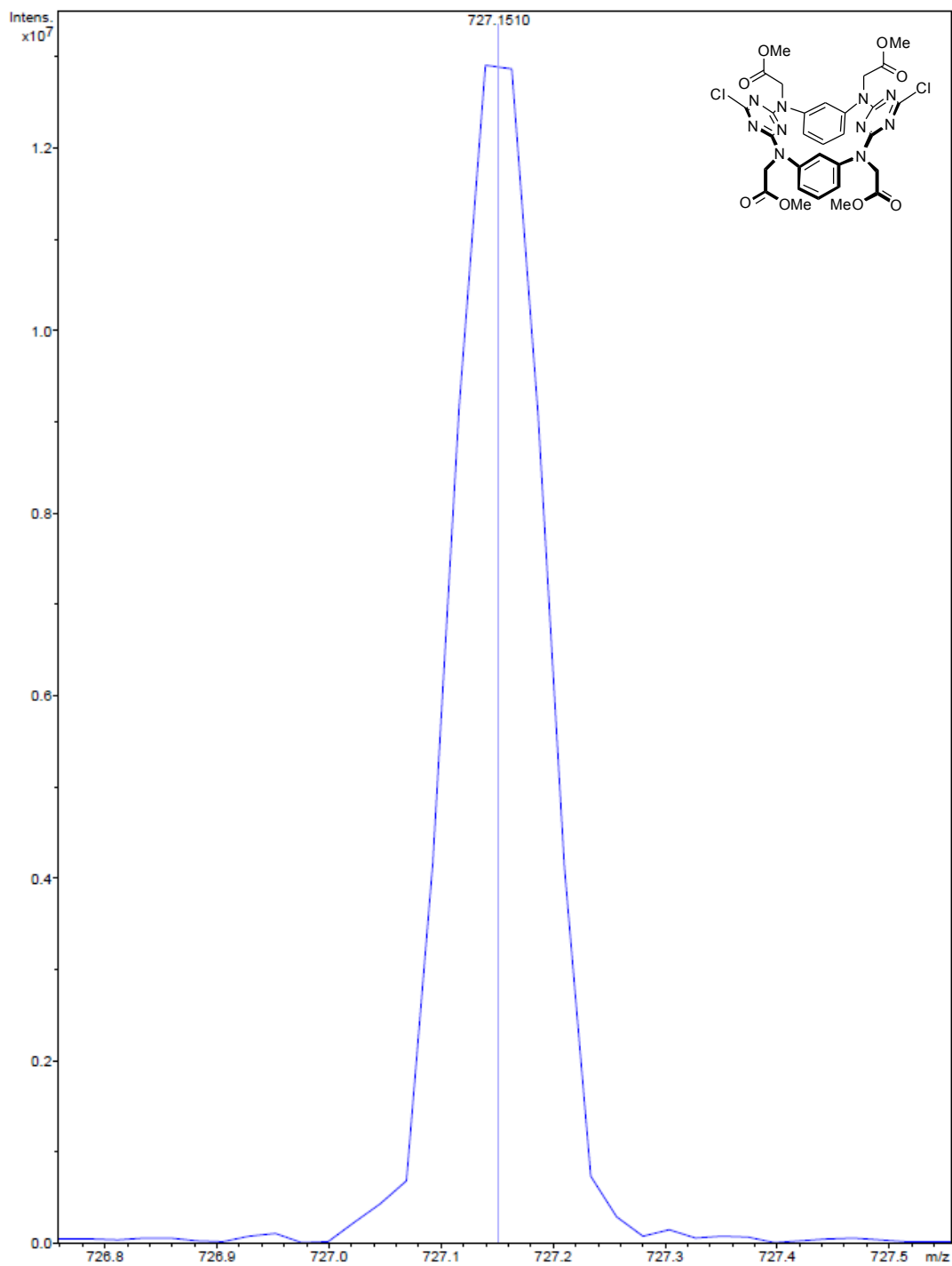


Figure S27. HRMS (ESI) spectrum of the $[M+H]^+$ of **1**.

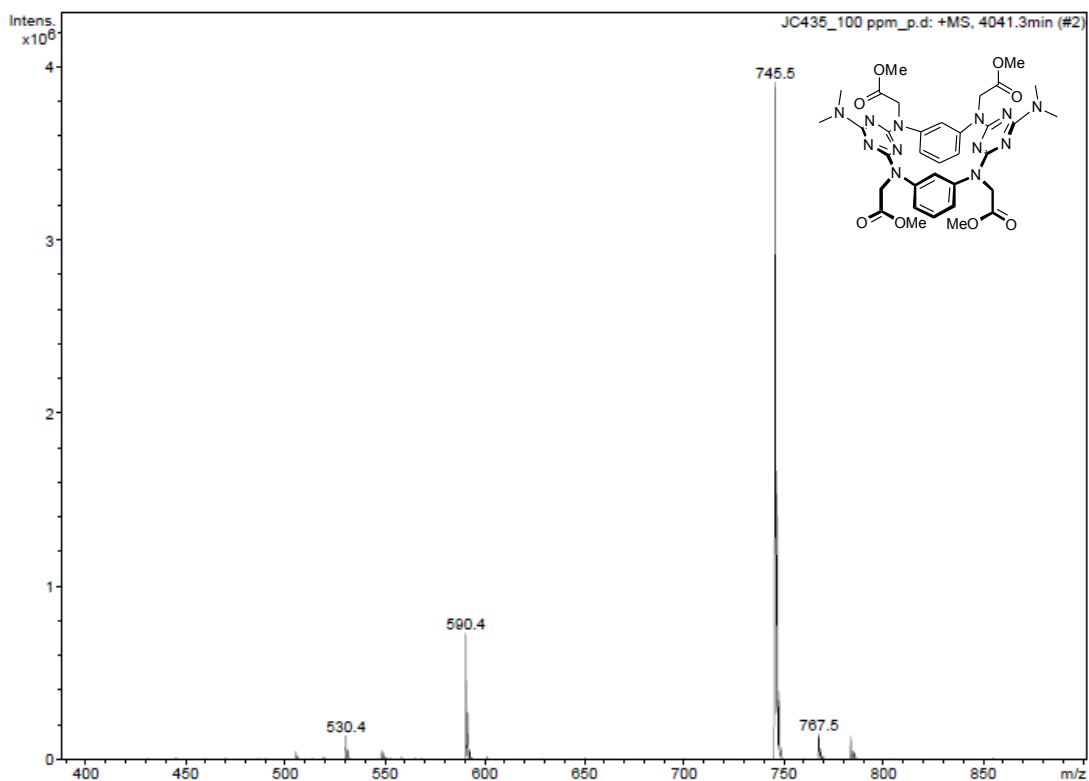


Figure S28. MS (ESI) spectrum of **2**.

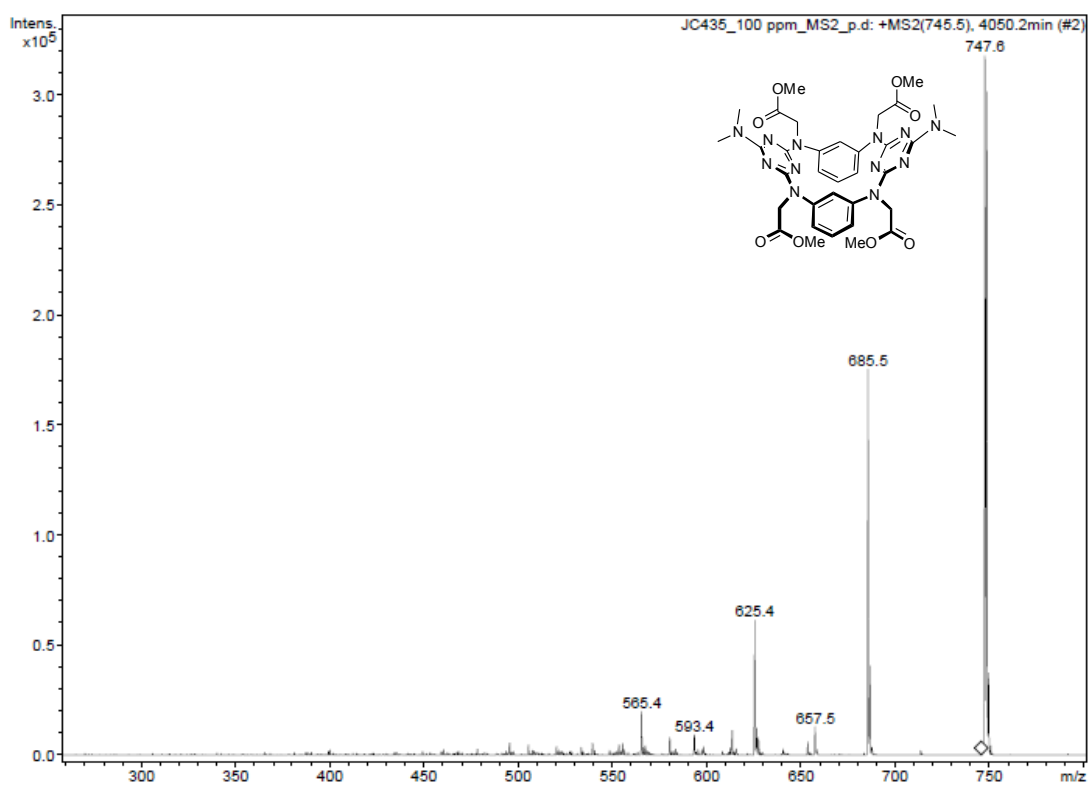


Figure S29. MS² spectrum of the [M+H]⁺ of **2**.

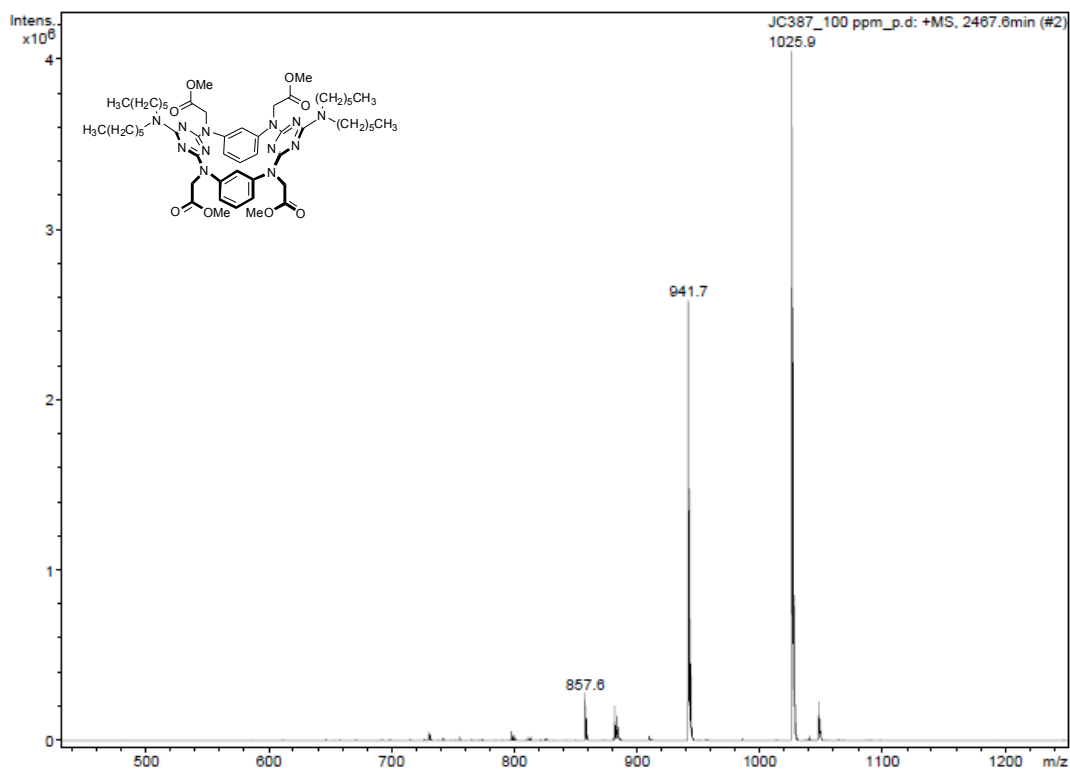


Figure S30. MS (ESI) spectrum of 3.

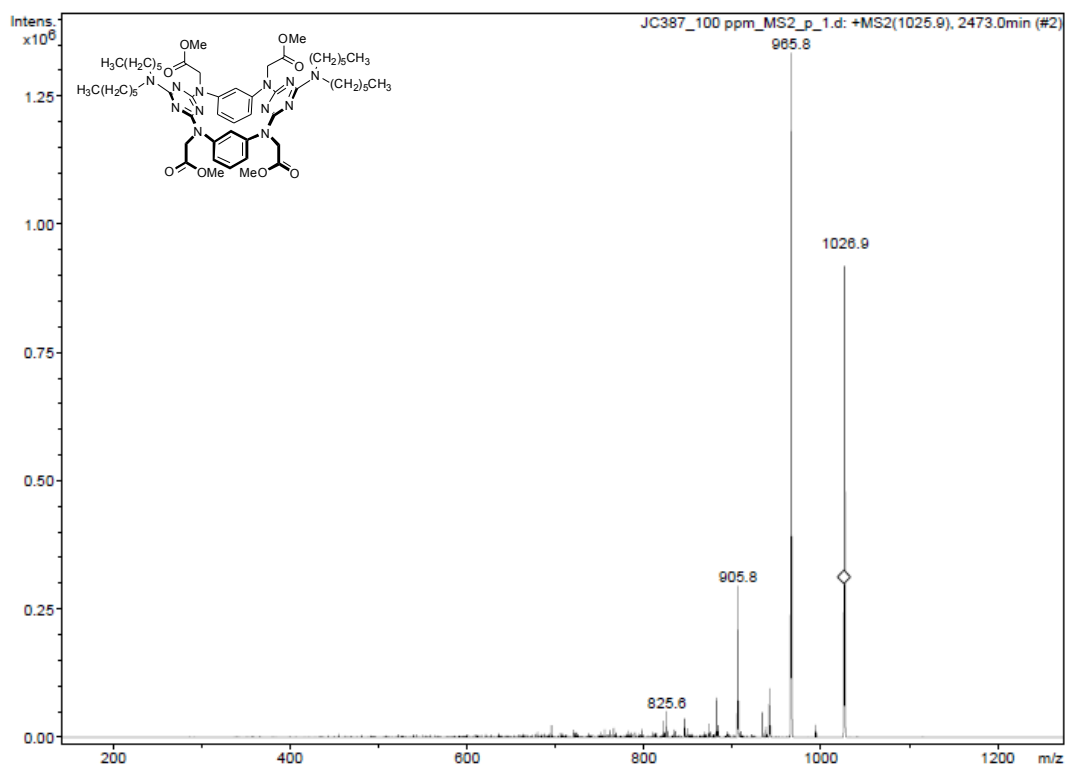


Figure S31. MS² spectrum of the $[M+H]^+$ of 3.

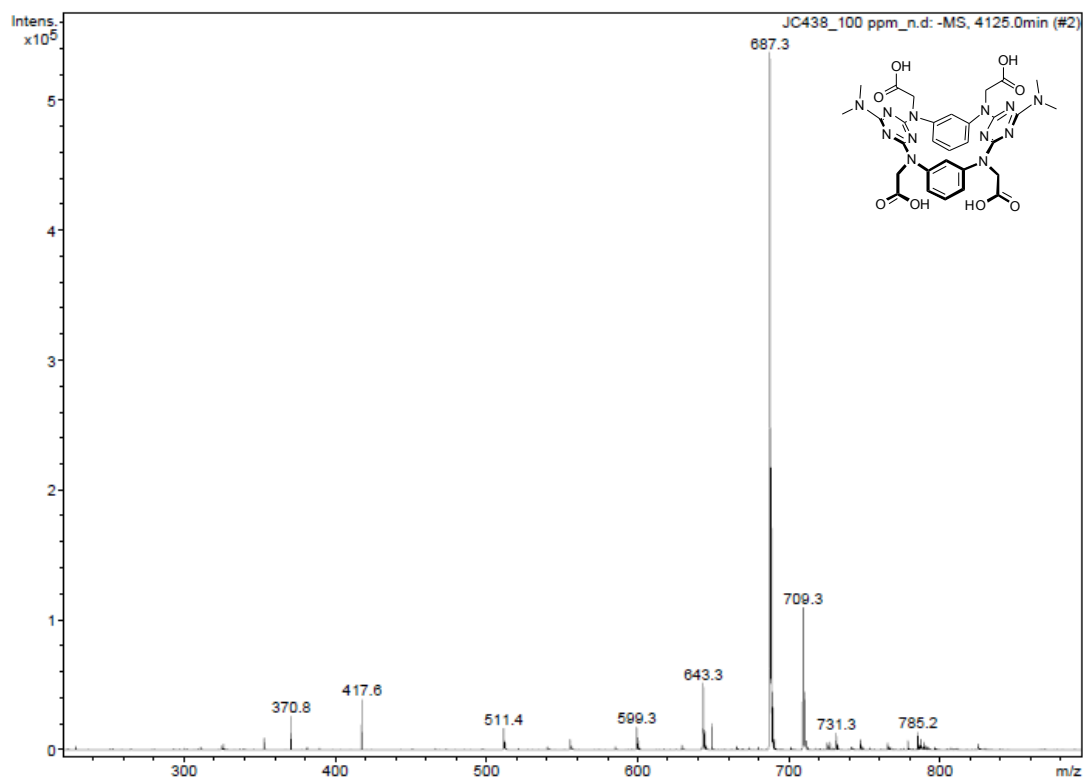


Figure S32. MS (ESI) spectrum of **4**.

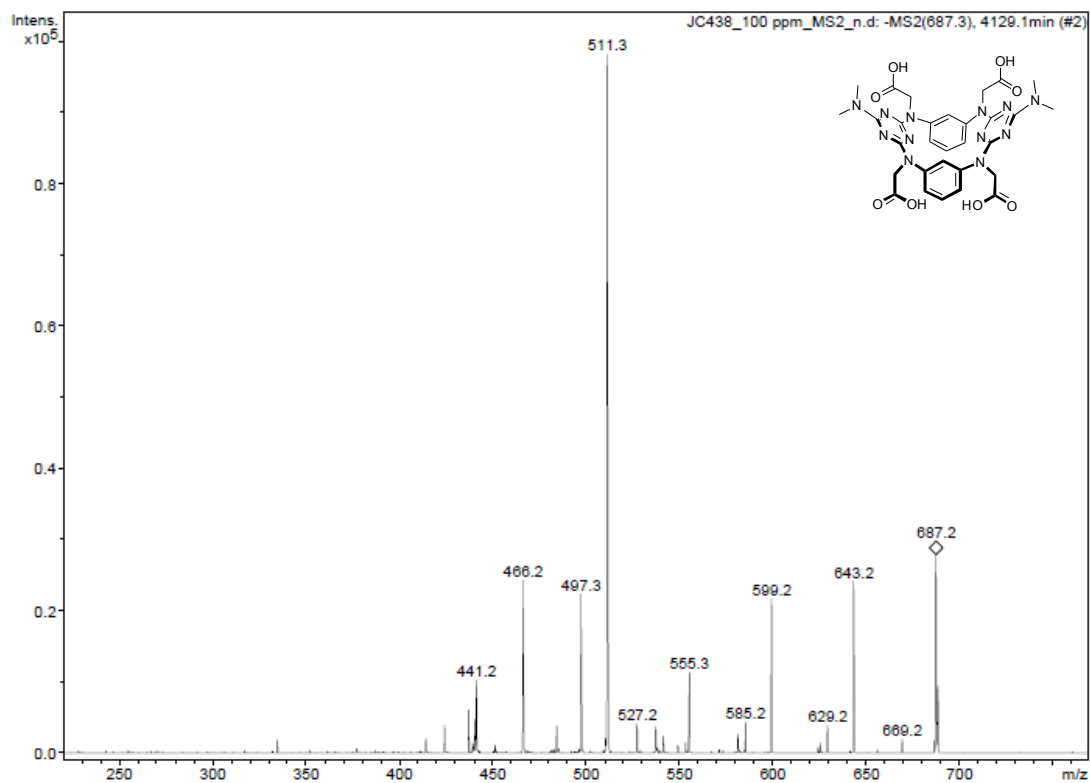


Figure S33. MS² spectrum of the [M+H]⁺ of **4**.

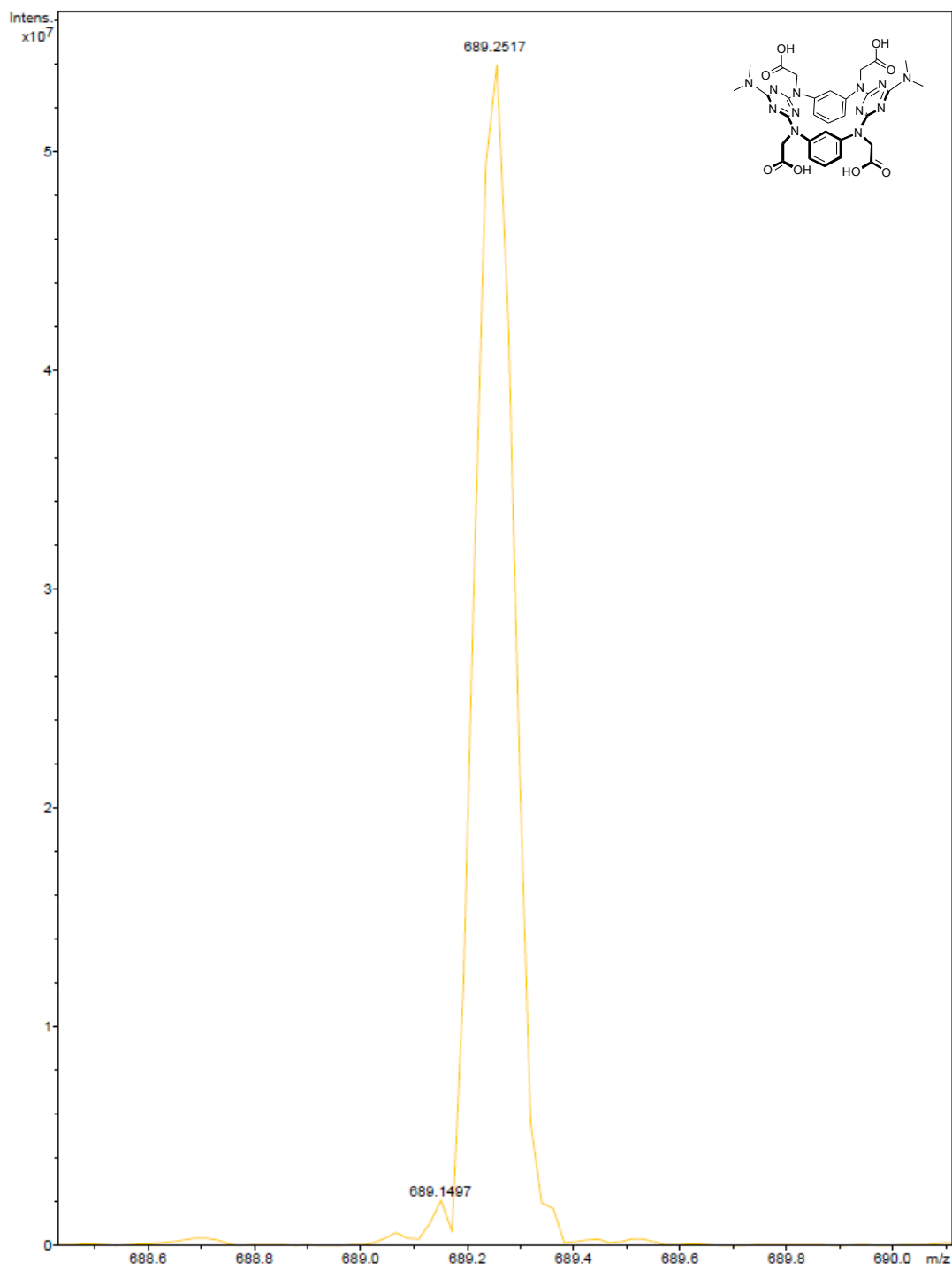


Figure S34. HRMS (ESI) spectrum of the $[M+H]^+$ of **4**.

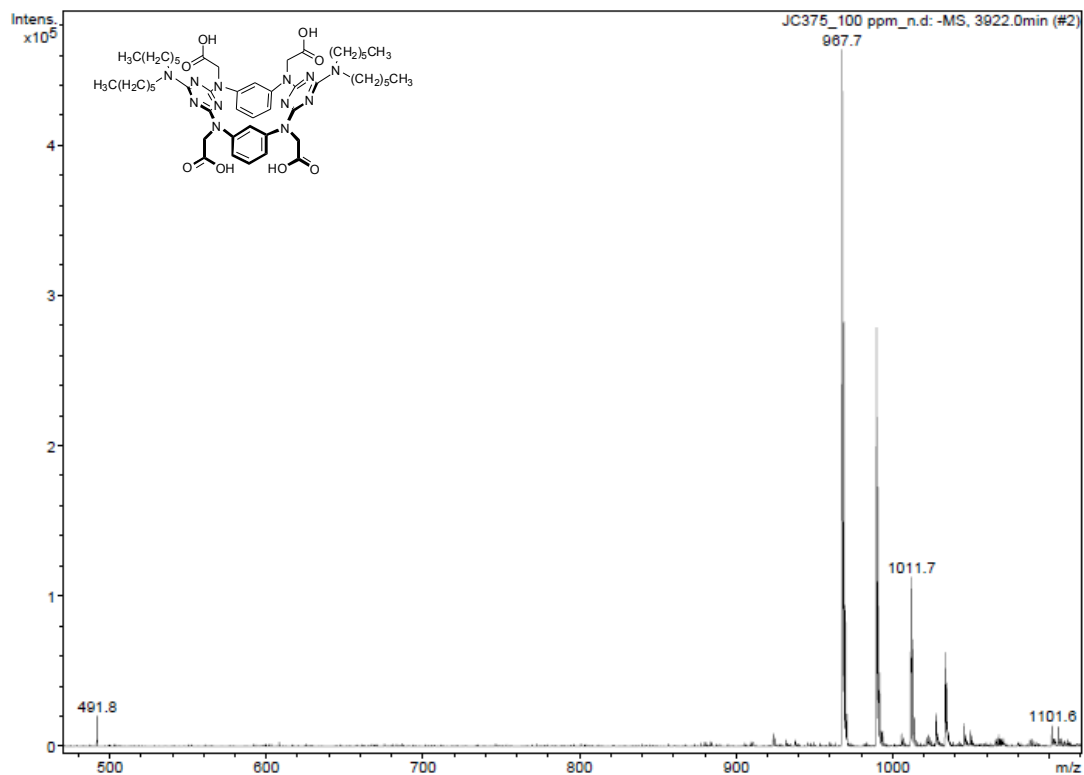


Figure S35. MS (ESI) spectrum of 5.

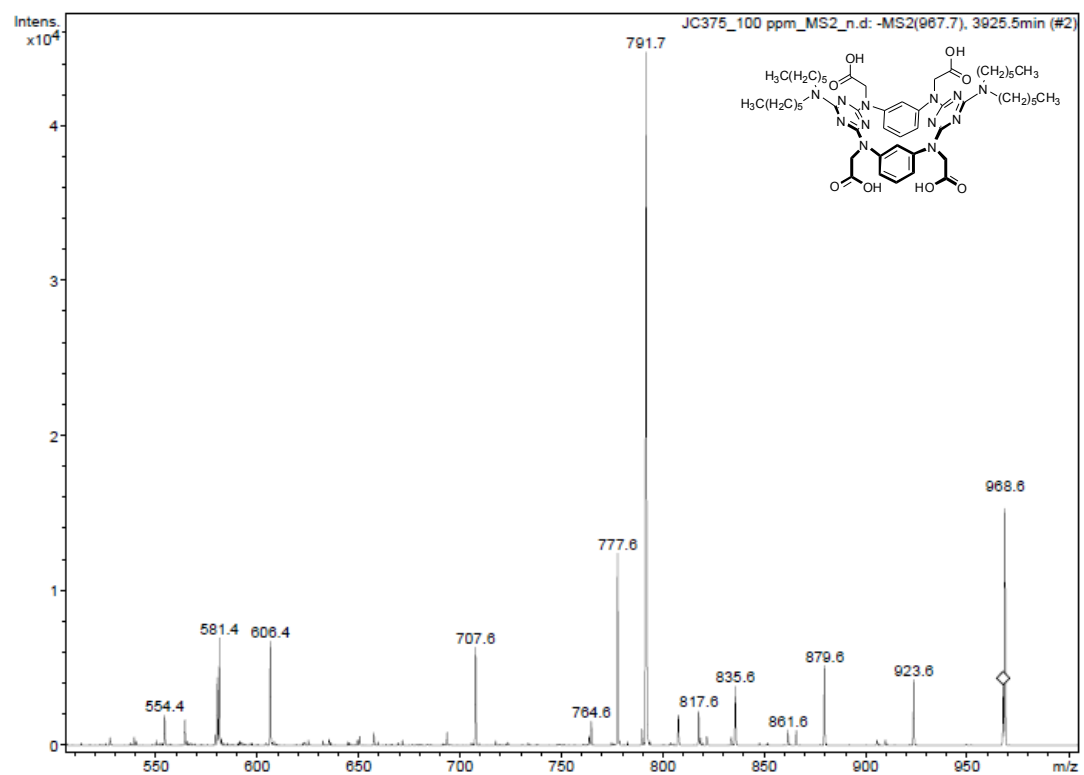


Figure S36. MS² spectrum of the [M+H]⁺ of 5.

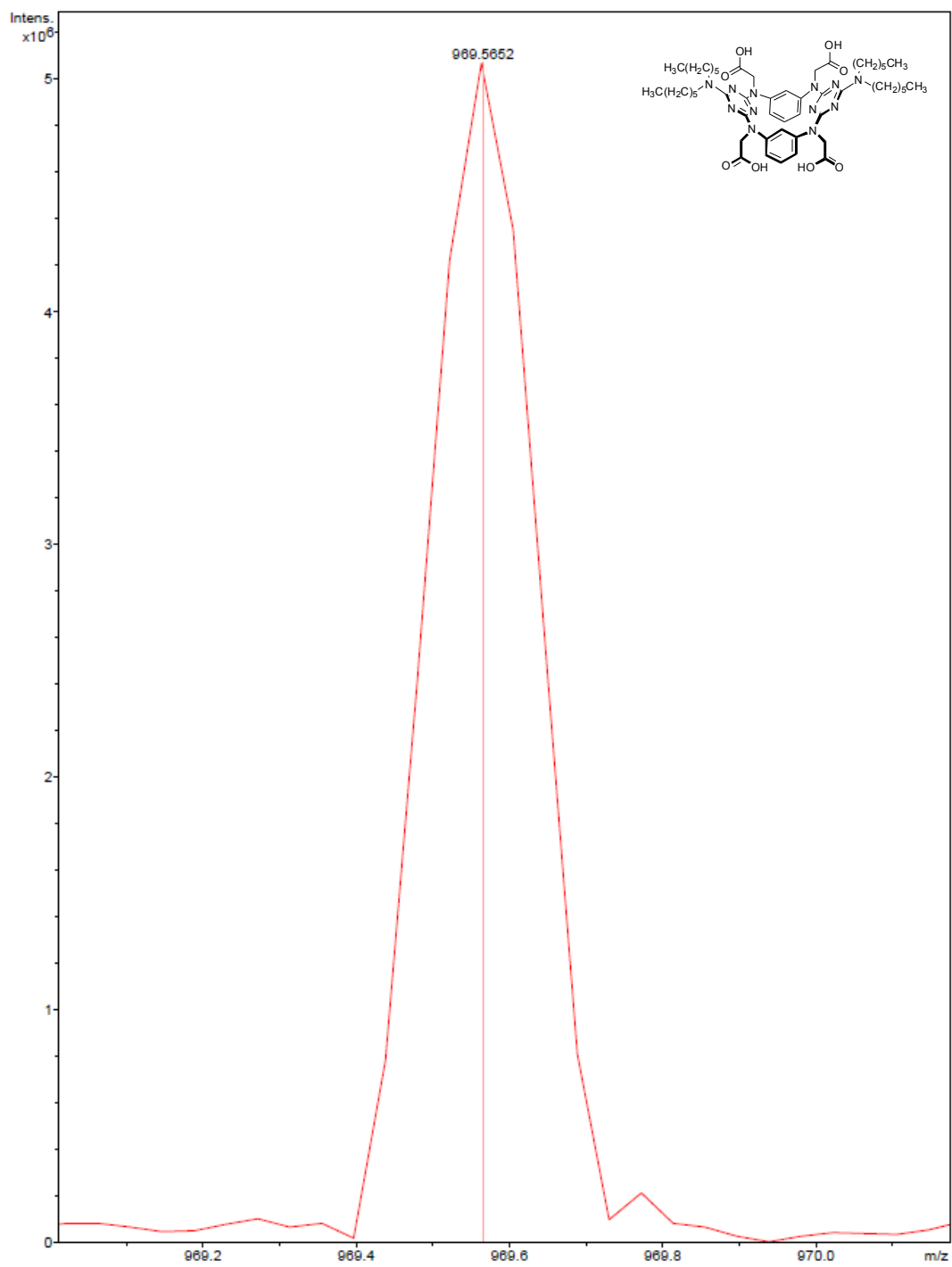


Figure S37. HRMS (ESI) spectrum of the $[M+H]^+$ of **5**.

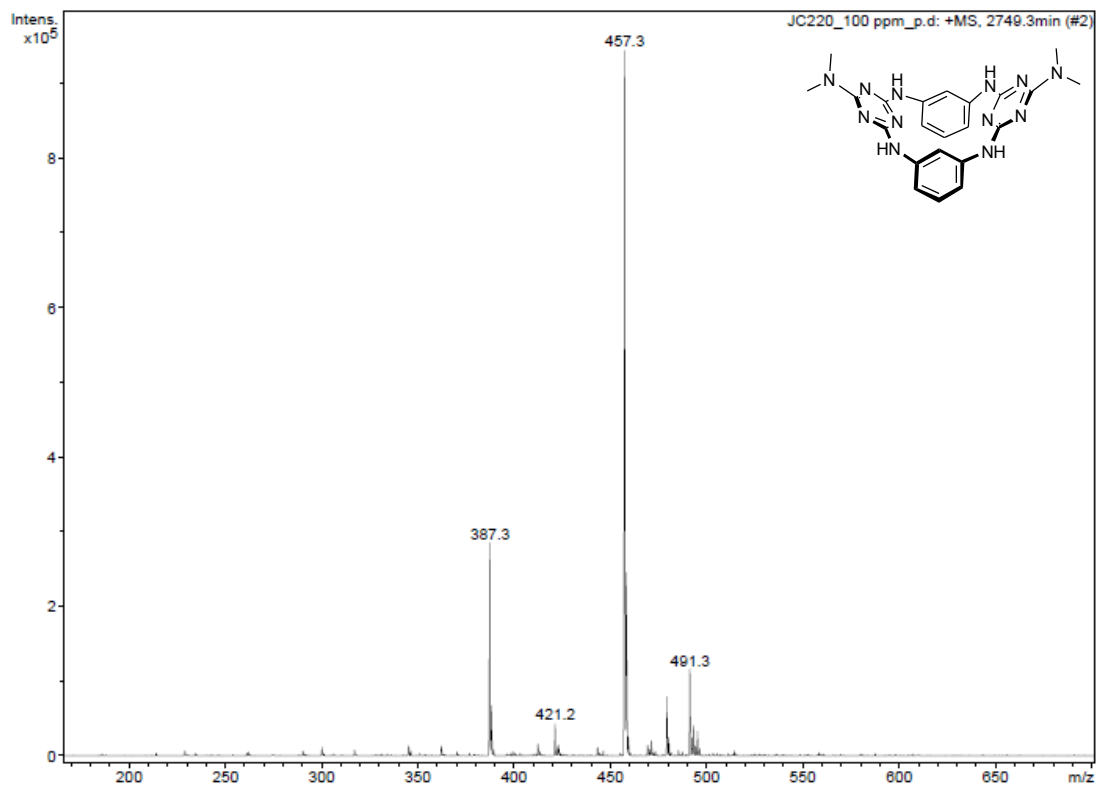


Figure S38. MS spectrum of 11.

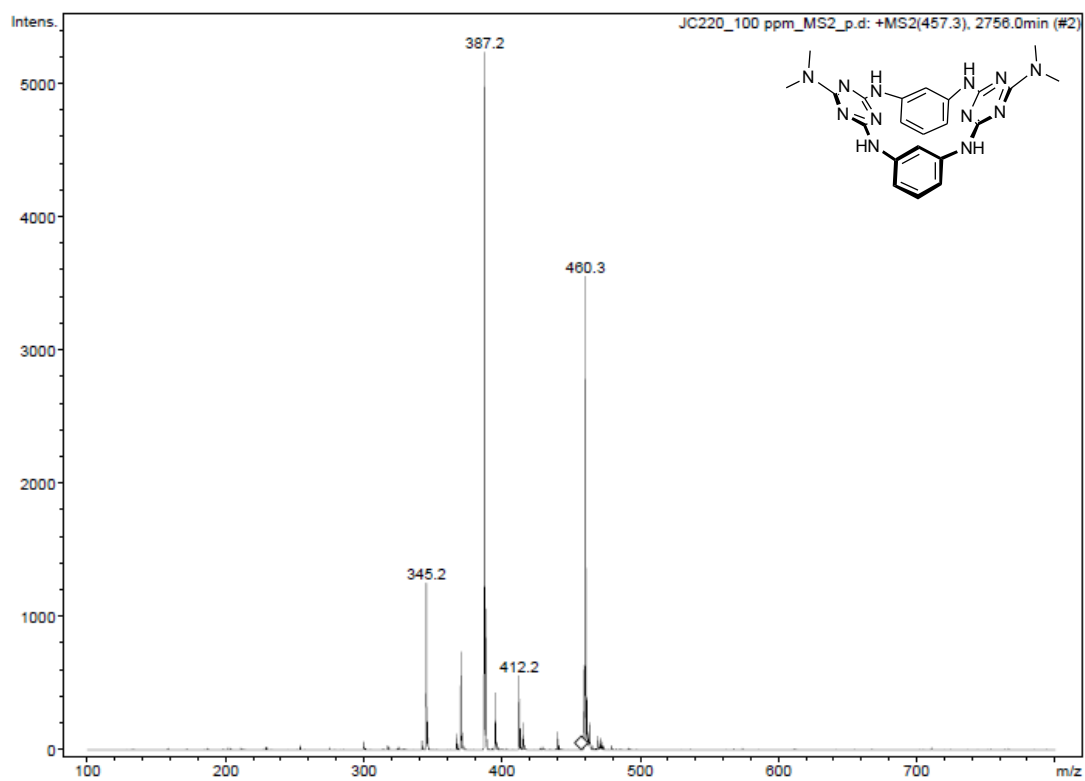


Figure S39. MS² spectrum of the [M+H]⁺ of 11.

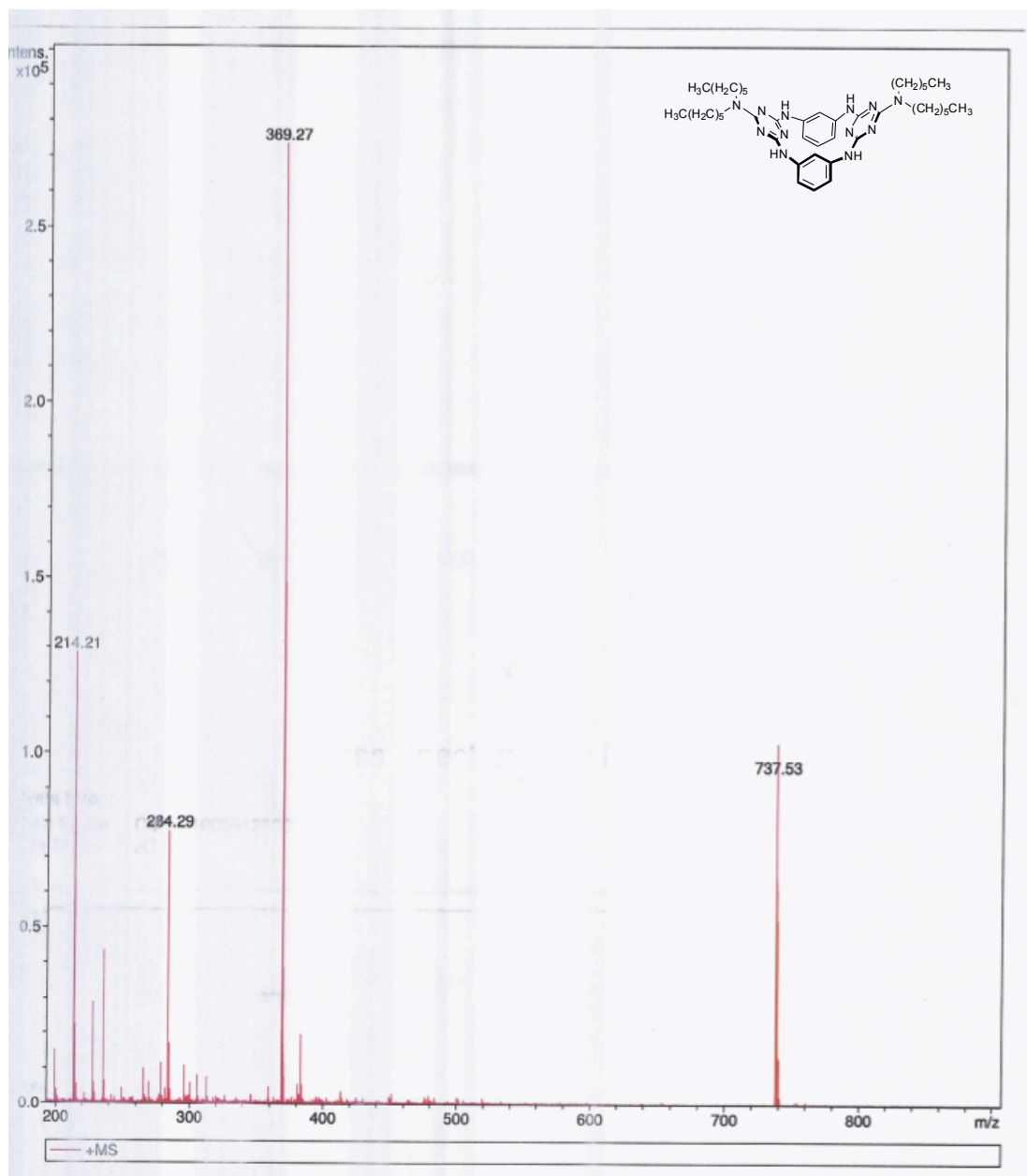


Figure S40. MS spectrum of 12.

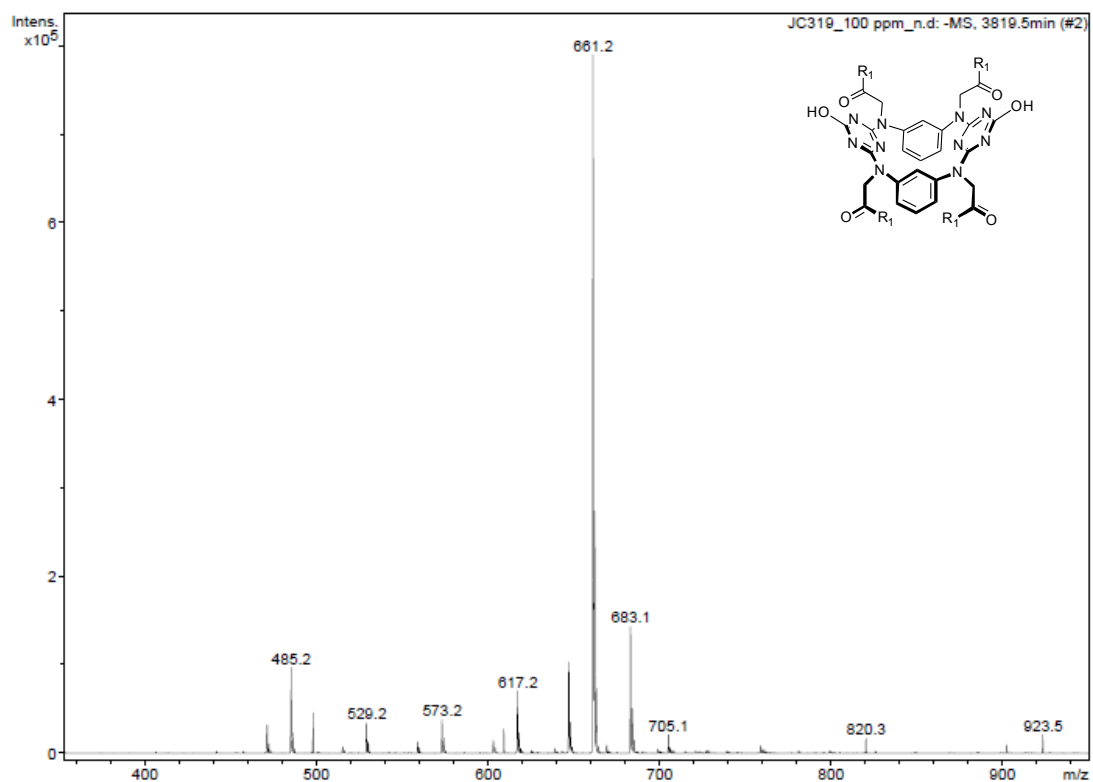


Figure S41. MS (ESI) spectrum of 13.

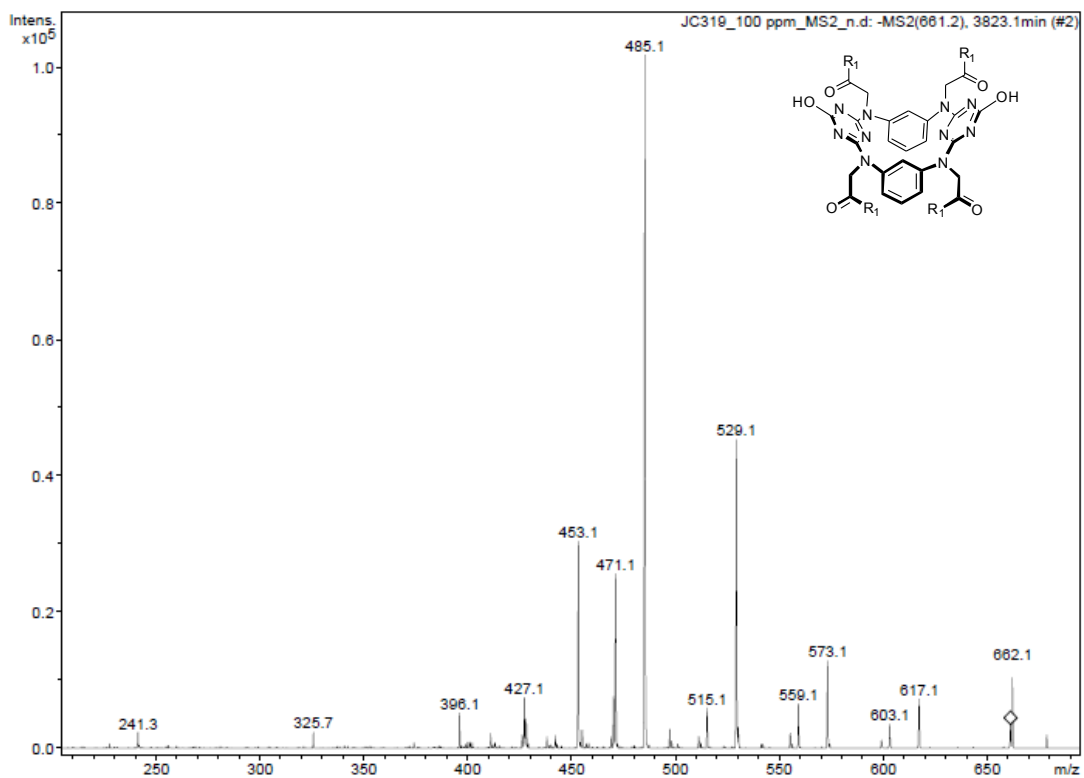


Figure S42. MS² spectrum of the [M+H]⁺ of 13.

UV-vis Titration

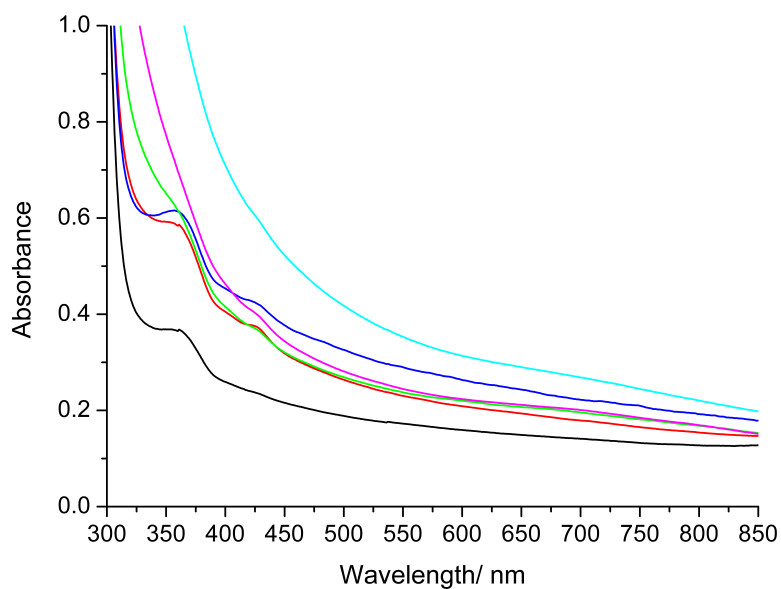


Figure S43. UV-vis titration of **4** (1.47×10^{-3} M) with Cu^{2+} in water, monitoring the metal absorption bands. UV-vis spectra were recorded at 20 °C with $\text{pH} \approx 11$ by the addition of increasing amount of CuCl_2 . The total concentrations of Cu^{2+} and ligand for curves, from bottom to top ranging between 0 and 1.30×10^{-3} M and 1.47×10^{-3} and 1.27×10^{-3} M, respectively.

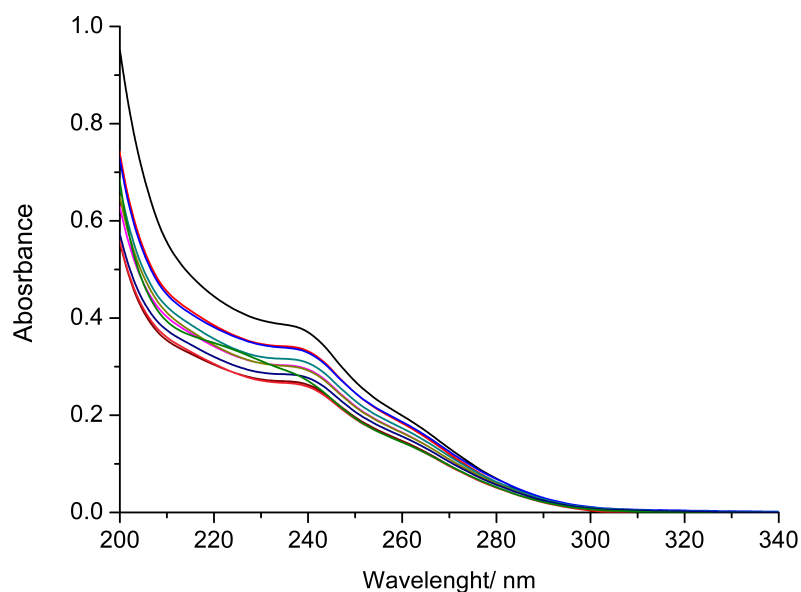


Figure S44. UV-vis titration of **4** (5.86×10^{-5} M) with Cu^{2+} in water, monitoring the ligand absorption bands. UV-Vis spectra were recorded at 20 °C with $\text{pH} \approx 11$ by the addition of increasing amount of CuCl_2 . The total concentrations of Cu^{2+} and ligand for curves, from bottom to top ranging between 0 and 5.71×10^{-5} M and 5.86×10^{-5} and 4.19×10^{-5} M, respectively.

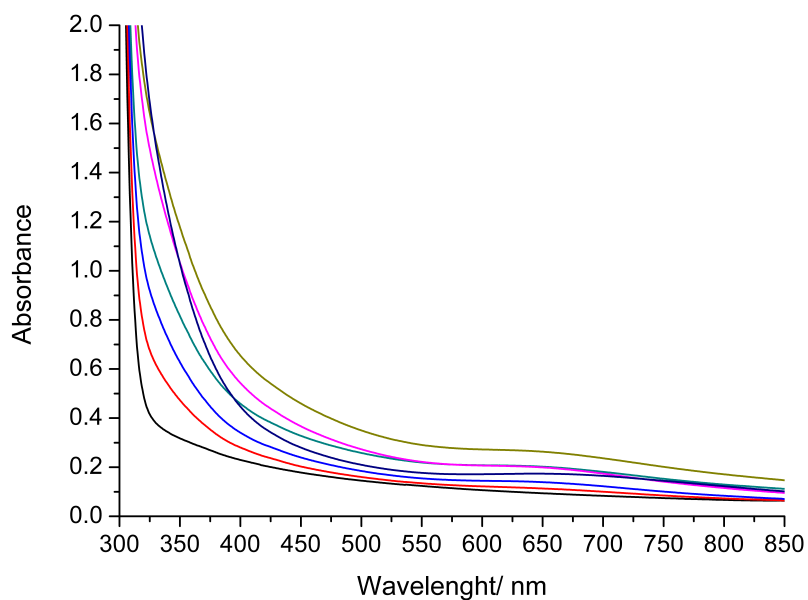


Figure S45. UV-vis titration of **5** (3.46×10^{-3} M) with Cu^{2+} in water, monitoring the metal absorption bands. UV-vis spectra were recorded at 20 °C with $\text{pH} \approx 11$ by the addition of increasing amount of CuCl_2 . The total concentrations of Cu^{2+} and ligand for curves, from bottom to top ranging between 0 and 2.65×10^{-3} M and 3.46×10^{-3} and 2.54×10^{-3} M, respectively.

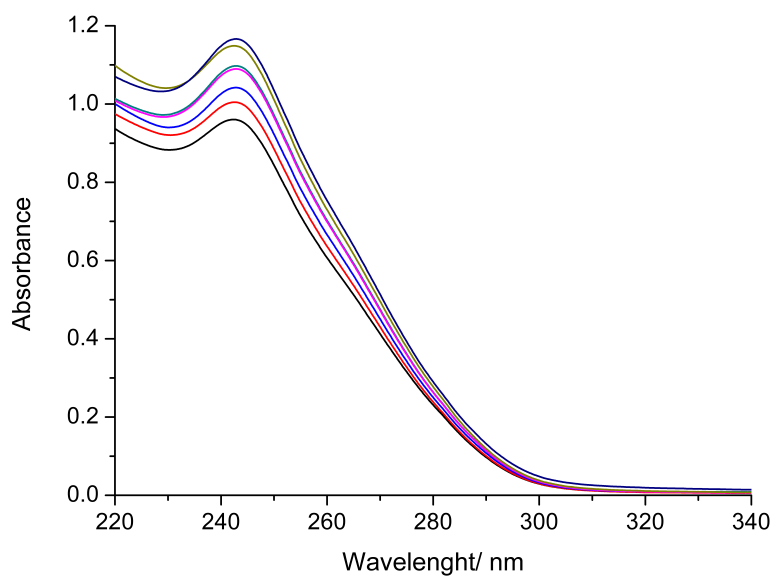


Figure S46. UV-vis titration of **5** (2.57×10^{-5} M) with Cu^{2+} in water, monitoring the ligand absorption bands. UV-vis spectra were recorded at 20 °C with $\text{pH} \approx 11$ by the addition of increasing amount of CuCl_2 . The total concentrations of Cu^{2+} and ligand for curves, from bottom to top ranging between 0 and 2.98×10^{-5} M and 2.57×10^{-5} and 2.19×10^{-5} M, respectively.

Crystallographic data

Table S1. Structural comparison of the tetraazacalix[2]arene[2]triazine scaffold in macrocycles **1**, **2** and **12**.

Macrocyle	C-N _{bridge, triazine} ^a	C-N _{bridge, phenyl} ^a	C-N _{bridge} -C ^b	Ω ^{b,c}	ϕ ^{b,c}	H _{ortho} ...H _{ortho} ^{a,d}	H _{meta} ...H _{meta} ^{a,d}
1 ^e	1.442(2)-1.444(2)	1.349(2)-1.358(2)	119.8(1), 120.0(1)	88.2	33.7	4.49	4.80
2	1.432(3)-1.440(3)	1.368(3)-1.371(3)	121.5(2)-122.4(2)	68.3, 71.4	35.2, 36.0	3.70	6.77
12	1.414(3) - 1.416(3)	1.355(3)-1.360(3)	132.2(2)-133.1(2)	25.8, 28.2	3.8, 4.3	2.75	11.54

^aAll distances are in Å. ^bAll angles are in deg. ^c Ω and ϕ Dihedral angles definition is given in the main text. ^dThe H_{ortho}...H_{ortho} and H_{meta}...H_{meta} distances are defined in the main text. ^e **1** Contains a 2-fold crystallographic axis.

Table S2. Crystal data and selected refinement details for macrocycles **1**, **2** and **12**.

Molecular formula	1 •diglyc	2 •THF	12 •2CHCl ₃
Empirical Formula	C ₃₆ H ₃₈ Cl ₂ N ₁₀ O ₁₃	C ₃₈ H ₄₈ N ₁₂ O ₉	C ₄₄ H ₆₆ Cl ₆ N ₁₂
M _w	889.66	816.88	975.78
Crystal System	Monoclinic	Triclinic	Monoclinic
Space group	<i>C2/c</i>	<i>P</i> $\bar{1}$	<i>P2</i> ₁ / <i>c</i>
<i>a</i> / Å	12.2611(11)	10.6377(4)	11.5804(7)
<i>b</i> / Å	18.2064(13)	12.7007(5)	14.7466(9)
<i>c</i> / Å	17.7004(19)	15.6556(7)	29.1684(19)
α / °	(90.0)	96.879(2)	(90)
β / °	100.734(4)	90.055(2)	90.758(2)
γ / °	(90.0)	106.439(2)	(90)
<i>V</i> / Å ³	3882.1(6)	2012.75(14)	4980.7(5)
<i>Z</i>	4	2	4
ρ_{calc} / mg mm ⁻³	1.522	1.348	1.301
μ / mm ⁻¹	0.249	0.099	0.390
Reflections collected	23350	26416	25720
Unique reflections, [<i>R</i> _{int}]	5940, [0.0394]	9481, [0.0399]	10935, [0.0325]
Final <i>R</i> indices			
<i>R</i> ₁ , <i>wR</i> ₂ [<i>I</i> > 2 σ]	0.0444, 0.1005 [4218]	0.0642, 0.1894 [7100]	0.0579, 0.1670 [7179]
<i>R</i> ₁ , <i>wR</i> ₂ (all data)	0.0725, 0.1131	0.0854, 0.2073	0.0946, 0.2046

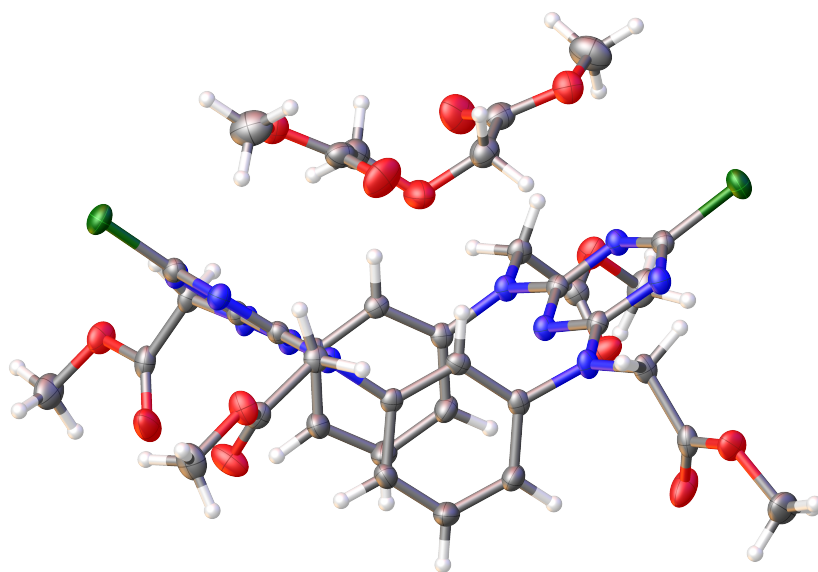


Figure S47. Molecular structure of **1•diglyc** with ellipsoids for non-hydrogen atoms drawn at the 50% probability level.¹

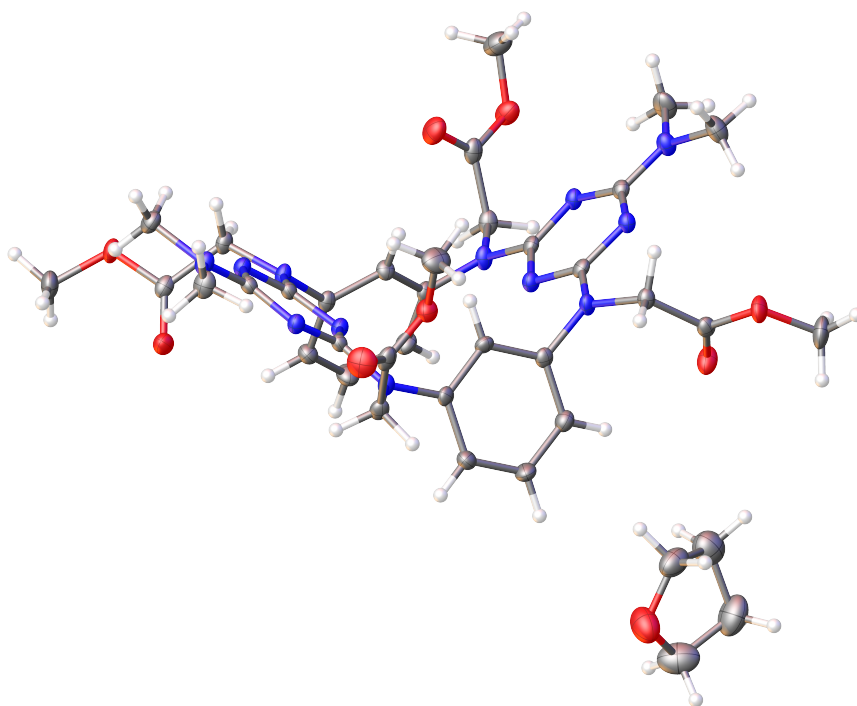


Figure S48. Molecular structure of **2.THF** with ellipsoids for non-hydrogen atoms drawn at the 50% probability level.¹

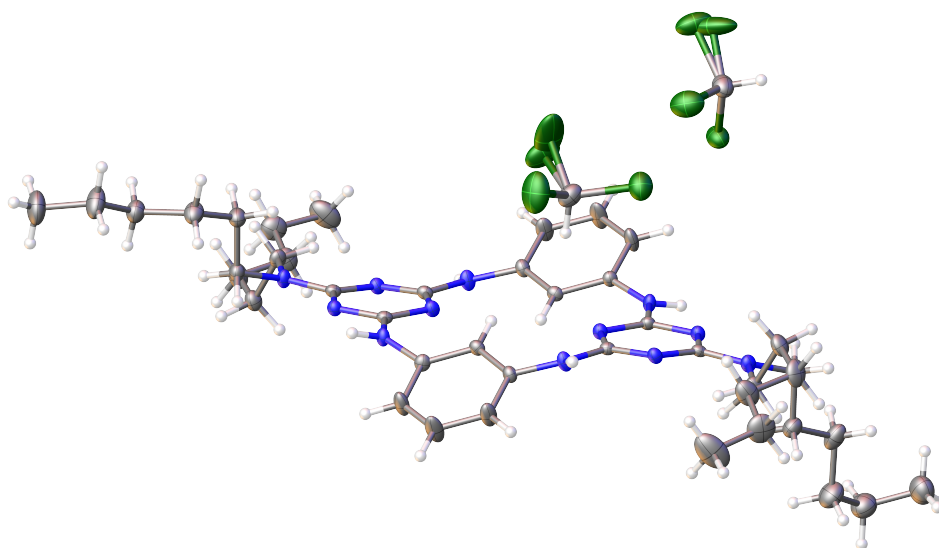


Figure S49. Molecular structure of 12.2CHCl_3 with ellipsoids for non-hydrogen atoms drawn at the 50% probability level.¹

Reference

- 1 O. V. Dolomanov, L. J. Bourhis, R. J. Gildea, J. A. K. Howard and H. Puschmann, OLEX2: a complete structure solution, refinement and analysis program, *J. Appl. Cryst.* **2009**, 42, 339–341.